minated. The water contained 0.25 mM of $NaHCO_3$, 0.25 mM of $CaCl_2$, 0.25 mM of $MgSO_4$, and 0.025 mM of $KHCO_3$ (pH 7.0; electrical conductivity, 145 μS/cm) (26).

Cell culture and virus. Human rhabdomyosarcoma cells (RD cells; NTCC CCL-136) were obtained from the American Tissue Culture Collection (Rockville, Md., U.S.A.) and grown in Dulbecco's modified Eagle's medium (D-MEM, Nissui Pharmaceutical, Tokyo) supplemented with 10% fetal bovine serum (FBS) at 37 C in an atmosphere containing 5% CO_2.

Poliovirus type 2 (Sabin strain) was kindly donated by Dr. H. Shimizu (Japan National Institute of Infectious Diseases, Tokyo). The virus was inoculated and propagated in RD cells using 2% FBS containing D-MEM for 3 days at 36 C in an atmosphere containing 5% CO_2 (24). After incubation, cells were lysed by freezing and thawing three times, followed by centrifugation at 10,000×g for 30 min at 4 C. The supernatant (virus suspension) was collected, divided into 1-ml aliquots, and stored at −80 C until needed.

Virus elimination system. A schematic representation of the virus elimination equipment is shown in Fig. 1. The system consisted of a glass column (internal diameter, 32 mm; length, 150 mm; Pyrex, Chiba, Japan), a pump (MW-901EEA; Enomoto Micro-pump, Tokyo), a glass gas-liquid separator (Pyrex), a storage tank (volume, 1 liter; Duran, Mainz, Germany), and a set of vinyl tubes (internal diameter, 10 mm; total length, 1.0 m). The anode was a carbon felt disk electrode (diameter 30 mm, thickness 10 mm; Nipponcarbon, Tokyo), in contact with a Pt-IrO_2-coated Ti conductive mesh plate (diameter 30 mm, thickness 1 mm; TDK, Tokyo). The carbon felt disk anode had been baked at 2,500 C, and its pores ranged from 10 to 200 μm in diameter. The cathode was another Pt-IrO_2-coated Ti mesh plate (diameter 30 mm, thickness 1 mm; TDK). A spongy polypropylene disc (diameter 29 mm, thickness 5 mm) and a round polypropylene ring (diameter 30 mm, thickness 5 mm) were placed between the anode and cathode, separating them by 5 mm. The solution was circulated axially through the columnar glass cell including the filter by the pump, at a flow rate of 200 ml/min. Current (1 or 10 mA) was applied to the electrodes by a power supply (Pan 160-0.4A, Kikusuidenshi, Tokyo). Hypochlorite concentration and pH were monitored continuously by a hypochlorite meter (Hach, Loveland, Colo., U.S.A.) and a pH meter (Horiba, Tokyo).

Measurement of the zeta potential of poliovirus. Polioviruses were diluted by modified tap water and filtrated through 0.2-μm of syringe filter (Millipore, Billerica, Mass., U.S.A.). Elecrophoretic mobility of poliovirus was measured by a laser microscopic electrophoresis method using 10^6 $TCID_{50}$/0.1 ml of poliovirus type 2 (Zeecom, Microtec Nition, Chiba, Japan) (18). Electrophoretic migration was observed under 40 V. Fifty poliovirus particles were observed microscopically in this experiment, and the zeta potential was calculated by the Smoluchowski equation (2).

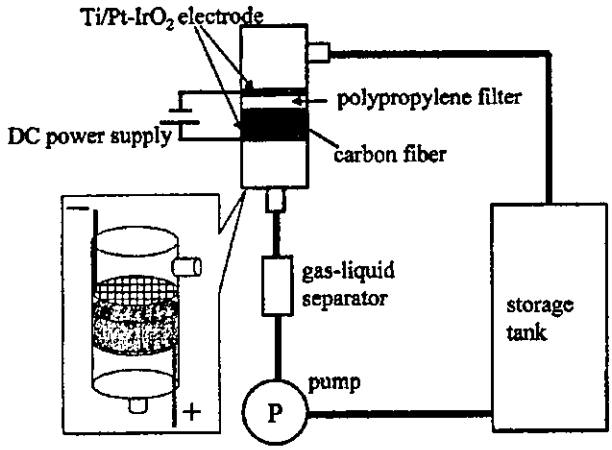

Fig. 1. Schematic illustration of our improved electrical removal system. The system includes columnar glass cell, pump, glass gas-liquid separator, storage tank, and vinyl tubing. The anode is a carbon felt disk filter, and the cathode is a mesh Pt-IrO_2-coated Ti plate. The solution is pumped through the filter, and the electric current is applied from a power supply unit. The solution was circulated through the glass columnar cell in an axial manner at a flow rate of 200 ml/min.

Indirect immunofluorescence assay for poliovirus. An indirect immunofluorescence assay for poliovirus was performed as previously described (22). Portions of the carbon felt electrode (approximately 100 pieces of felt) were collected from the surface of the disk during experiments. Samples were affixed to a thin slide glass (Matsunami, Tokyo) using a clear acryl adhesive (Shiseido, Tokyo). To prevent nonspecific reaction between the carbon felt electrode and the antibodies, 100 μl of PBS containing 1% bovine serum albumin (Sigma, St. Louis, Mo., U.S.A.) was placed upon the carbon felt samples and incubated in a humid chamber at 37 C for 45 min. After the felt was washed twice with PBS, 100 μl of anti-poliovirus type 2 mouse monoclonal antibody solution (dilution, 1:400; Chemicon, Temecula, Calif., U.S.A.) was placed upon the felt samples for incubation at 37 C for 45 min in the humid chamber. After incubation, excess antibody was removed by rinsing twice with PBS; then samples were stained with 100 μl of FITC-labeled anti-mouse IgG goat polyclonal antibody (1:200; Chemicon) at 37 C for 45 min. Then the samples were washed twice with PBS and air dried. Immunofluorescence was analyzed with a laser confocal

Table 1. Nucleotide sequences of primers and fluorogenic probes used for real-time quantitative RT-PCR used in this study

Primer or probe	Positions[a]	Nucleotide sequences (5'–3')
SB2-R1 (sense)	4468–4487	AGC AAG CAC CGT ATT GAG CC
SB2-F1 (antisense)	4687–4667	GTT TCA TGT CTG CTC CGT CTG
Polio-FL (fluorescein)[b]	4570–4596	GAG AAC ACC TCC ACA TAC TCA CTG CCA
Polio-FC (fluorophore)[c]	4598–4624	CTG ATC CGT CTC ACT TTG ATG GCT ACA

[a] Positions represent the VP2 gene sequences of the poliovirus type 2 (GenBank accession no. AY184220).

[b] Fluorescein was used to label the 3' end of the oligonucleotide.

[c] Fluorophore (LightCycler Red 640) was used to label the 5' end of the oligonucleotide.

microscope (Radiance 2100; BioRad, Tokyo).

Tissue culture infective dose (TCID) assay. We suspended 100 or 300 µl of aliquoted poliovirus in 1,000 ml of modified tap water. The poliovirus-suspended modified tap water was circulated through the system at room temperature (20 to 22 C). During circulation, we serially collected 5.0-ml samples at 0, 5, 15, 30, and 60 min from the storage tank of the system. Since low concentrations of oxidants such as hypochlorite may be generated by electrolysis, these were eliminated and solutions made isotonic by adding 1 ml of concentrated D-MEM (5×) supplemented with 10% FBS to samples. All collected samples were stored on ice. Bacterial contamination after sample collection was prevented by filtration through a 0.2-µm syringe filter (Millipore). The infective dose of poliovirus was measured by a cell culture method using RD cells in 96-well micro titer plates (Corning, Corning, N.Y., U.S.A.) (24). Cytotoxic effects from poliovirus were observed over 7 days using a phase-contrast microscope. The 50% tissue culture infective dose ($TCID_{50}$) was calculated as described previously (23). Viral density in the original poliovirus suspension was about 1.5×10^7 $TCID_{50}$/0.1 ml.

RNA extraction, reverse transcription (RT), and quantitative real-time polymerase chain reaction (PCR). Since poliovirus might be inactivated by the electric current in the trapping chamber, the poliovirus VP2 gene was quantitated in samples using modified real-time PCR as previously described (15). Briefly, poliovirus RNA was extracted from 140 µl of sample using a QiAmp Viral RNA Mini Kit (Qiagen, Hilden, Germany). Fifteen microliters of DNase I-treated RNA solution was added to 15 µl of RT solution containing 100 mM Tris-HCl at pH 8.3, 150 mM KCl, 6 mM $MgCl_2$, 1 mM of dNTP mixture, 10 mM dithiothreitol, 75 pmol of random hexamer (TaKaRa, Tokyo), 30 units of RNase inhibitor (TaKaRa), and 200 units of reverse transcriptase [Superscript II, RNaseH (−); Invitrogen, San Diego, Calif., U.S.A.]. This RT mixture was incubated at 42 C for 50 min, and then at 99 C for 15 min. After RT we performed quantitative real-time PCR. A 220-bp portion of the VP2 gene from the poliovirus type 2 (Sabin strain) including bases 4468 to 4687 (GenBank accession number X00595) was amplified using specific primers (Table 1). We designed a new set of hybridization probes to label this partial VP2 gene from poliovirus for quantitative PCR method using a commercially available system (Light Cycler, Roche Molecular Biochemicals, Mannheim, Germany). These fluorogenic probes, also presented in Table 1, were labeled at the 5' end with Light Cycler Red 640 fluorophore and at the 3' end with fluorescein (Nihon Gene Research Laboratory, Miyagi, Japan). The real-time PCR mixture contained 5 µl of 3-fold diluted sample RT product (cDNA), 2 µl of probe mixture (Master Hybridization Probes Reaction Mix, Roche Molecular Biochemicals), 1 µl (10 µmol) of primers SB2-R1 and SB2-F1, 2 µl (2 µmol) of probes Polio-FL and Polio-LC, 2.4 µl of $MgCl_2$ (final concentration, 4 mM), and PCR-grade sterile water to a final volume of 20 µl. The following PCR protocol was used: a 10-min denaturation step at 95 C, followed by 45 repeated cycles of denaturation (10 sec at 95 C), annealing (10 sec at 56 C), and polymerization (10 sec at 72 C). The temperature transition rate was 20 C/sec in all segments. Following amplification, melting curve analysis was performed with a heating rate of 0.2 C/sec starting at 63 C. Fluorescence values for each capillary were measured at 640 nm. Amplification data were collected and analyzed with software for the system (Light Cycler Software version 3.5, Roche Molecular Biochemicals). A standard for confirming copy numbers of poliovirus type 2 VP gene was set up by 10-fold serial dilution (10^6 to 10 copies/5 µl) of purified cDNA (220 bp) assessed by ultraviolet (UV) -photometry at λ=260 nm.

Statistical analysis. Raw values or normalized values from the indicated number of independent trials were averaged and expressed as the mean±standard error (SE). Statistical significance of the difference between various treatments groups was assessed with paired or unpaired Student's *t* test.

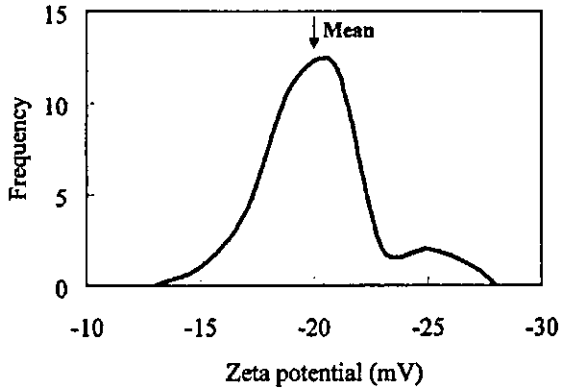

Fig. 2. Frequency distribution of zeta potential of polioviruses in modified tap water. Approximately 10^6 $TCID_{50}$/0.1 ml of poliovirus suspension was used. Zeta potential of polioviruses was measured by laser microscopic electrophoresis.

Results

Zeta Potential of Poliovirus

Zeta potential is generated by solid-liquid surface interactions (12, 31). When suspended in an ionic solution, some biologic particles such as bacteria and viruses spontaneously become negatively charged (12, 31). Particles with stronger negative charges are adsorbed more readily to a positively-charged carbon felt electrode. The zeta potential of polioviruses suspended in modified tap water was measured by a laser microscopic electrophoresis method based on the electrophoretic mobility of virus particles. In this study, 10^6 $TCID_{50}$/0.1 ml of poliovirus was used as a sample. The frequency distribution of zeta potential of polioviruses in modified tap water, shown in Fig. 2, ranged from −13 to −27 mV in this study. The mean zeta potential of polioviruses was approximately −20 mV.

Electroadsorption of Poliovirus to the Carbon Felt Electrode

To determine whether a positively-charged carbon felt electrode effectively adsorbed poliovirus particles, we performed an indirect immunofluorescence assay to detect poliovirus on the electrode using 4,000 $TCID_{50}$/0.1 ml of virus suspension. The virus particles would be expected to be adsorbed on contact with the carbon felt electrode. The virus suspension was circulated through the columnar glass cell containing the electrode, at a flow rate of 200 ml/min. We serially collected approximately 100 pieces from the surface of the carbon felt electrode during experiments. Results of the immunofluorescence assay for polioviruses are shown in Fig. 3. Significant immunofluorescence from the carbon felt electrode was detected at 10 mA at 60 min of circulation (Fig. 3A). Immunofluorescence was not

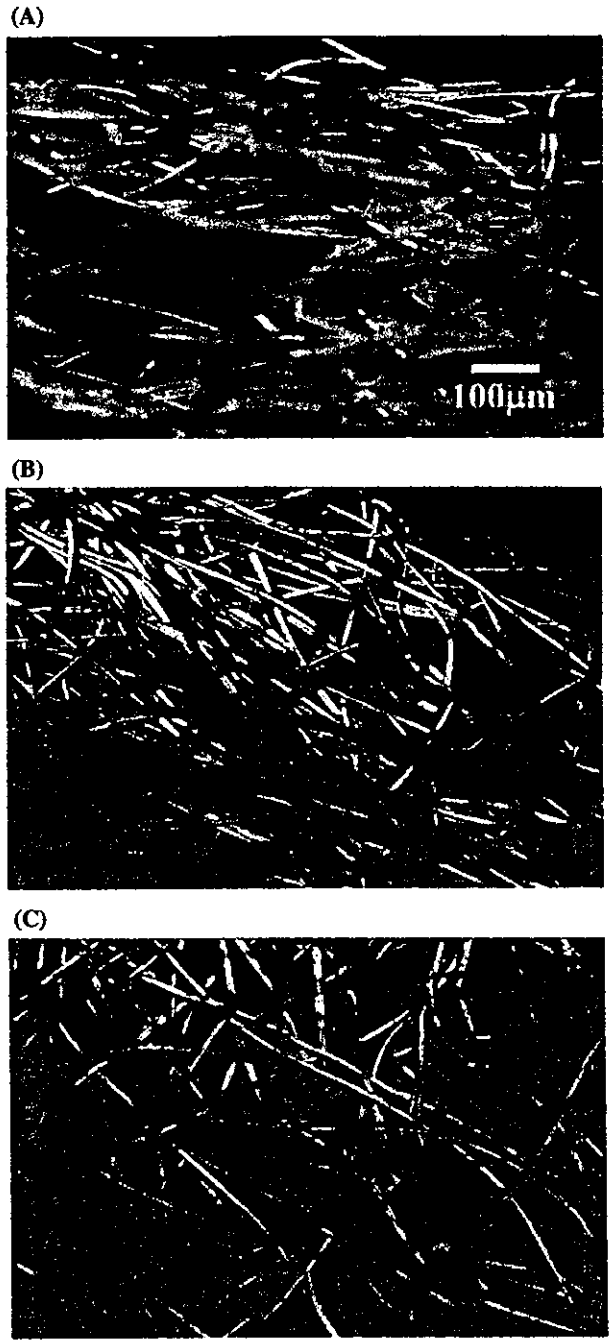

Fig. 3. Adsorption of polioviruses to the carbon felt electrode. Immunofluorescence derived from FITC-labeled antibody to virus was analyzed using a laser confocal microscope. A: A carbon felt electrode used to treat modified tap water containing 4,000 $TCID_{50}$/0.1 ml of poliovirus at 10 mA for 60 min of circulation. B: A carbon felt electrode used to treat modified tap water containing 4,000 $TCID_{50}$/0.1 ml of poliovirus at 0 mA (no electric current) for 60 min of circulation. C: Control carbon felt electrode exposed to modified tap water lacking poliovirus at 10 mA for 60 min of circulation. Bar indicates 100 μm.

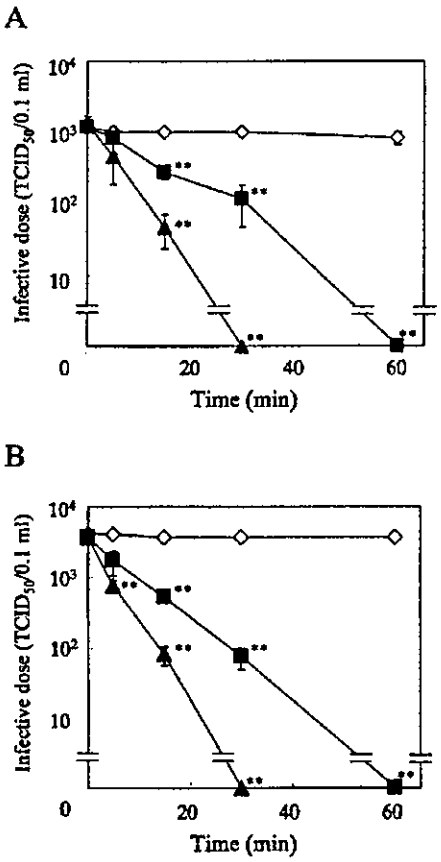

Fig. 4. Time course of decrease in TCID of poliovirus. Experimental conditions were 1,000 $TCID_{50}$/0.1 ml of poliovirus (A) or 4,000 $TCID_{50}$/0.1 ml of poliovirus (B). TCID was assayed by a cell culture method using human rhabdomyosarcoma cells (RD cells). ◇, mean TCID at 0 mA (no electric current); ■, at 1 mA; ▲, at 10 mA. Vertical bar indicates the standard error (SE) of triplicate experiments. $*P<0.05$ vs. control, $**P<0.01$ vs. control.

detected at 0 mA (no current) at 60 min of circulation (Fig. 3B). No fluorescence was observed from the control (no virus; 0 mA for 0 min of circulation, Fig. 3C). These results suggested that polioviruses were effectively adsorbed to the positively-charged carbon felt electrode.

Elimination of Poliovirus According to Tissue Culture Infective Dose (TCID)

Similar experiments were carried out using both 1,000 and 4,000 $TCID_{50}$/0.1 ml of poliovirus type 2. We serially collected 5.0-ml samples from the storage tank of the system. Infective dose assay of poliovirus was performed with a cell culture method using RD cells. Elimination of poliovirus is shown by TCID in Fig. 4. For both 1,000 and 4,000 $TCID_{50}$/0.1 ml poliovirus suspensions, no poliovirus was detected after treatment with 10 mA (voltage, 8.5 V) for 30 min of circulation in the system. No poliovirus was detected after 1 mA (voltage, 2.5 V) for 60 min of circulation. Decreases in TCID for lesser exposure to the system showed dependence on electric current and time. At 0 mA (no electric current) for 60 min of circulation, TCID was not significantly decreased. When the carbon felt disk was omitted from the system, TCID was not changed by 10 mA for 60 min of circulation (data not shown). Essentially no hypochlorite was generated (less than 0.02 mg/liter), and pH did not change during experiments (data not shown). Accordingly, relatively high concentrations of infective poliovirus (about 4,000 and 1,000 $TCID_{50}$/0.1 ml) were removed effectively by the positively-charged carbon felt electrode.

Quantitation of the Poliovirus VP2 Gene

Table 2 shows determinations of poliovirus VP2 gene copy numbers in samples. Experimental conditions were as same as for Fig. 4. Sensitivity limits for detection of the poliovirus VP2 gene were 100 copies/0.1 ml of sample (data not shown). First, significant decreases in poliovirus genome were noted in samples treated with 10 mA for 30 min of circulation; any copies present were below the limit of sensitivity. Additionally, at 1 mA for 60 min, the poliovirus genome was not detected, suggesting that polioviruses were removed effectively by longer exposure to a low current. The electrode did not significantly adsorb viruses at 0 mA for 60 min of circulation (Fig. 3B). By this quantitation method as well, the positively-charged electrode effectively adsorbed the viruses.

Discussion

We demonstrated that a positively-charged carbon felt electrode could effectively adsorb relatively high concentrations of poliovirus type 2, eliminating the viruses from modified tap water. The results suggest that our method could effectively remove certain viruses contaminating the water. Most bacteria and viruses are negatively charged in water (12), and our results suggest that poliovirus type 2 also is negatively charged (zeta potential, about −20 mV). Such negatively charged virus particles would be likely to adsorb to a positively-charged electrode such as our carbon felt electrode (1). Adsorption and elimination of polioviruses depended on the strength of electric current in our system (Figs. 3 and 4). At 10 mA, a relatively high concentration of poliovirus (4,000 $TCID_{50}$/0.1 ml) was removed completely from the water after 30 min of treatment by our system. In contrast, at no current (0 mA), the polioviruses were not adsorbed on the carbon felt. This suggests that elimination of polioviruses in this study

Table 2. Quantitation of the poliovirus VP2 gene

Infective dose ($TCID_{50}$/0.1 ml)	Electric current (mA)	Time (min) 0	5	15	30	60
1,000	0	$1.3\times10^3\pm5.8\times10$	$1.3\times10^3\pm5.8\times10$	$1.2\times10^3\pm4.4\times10$	$1.2\times10^3\pm3.3\times10$	$1.0\times10^3\pm3.3\times10$
	1	$1.2\times10^3\pm5.8\times10$	$1.0\times10^3\pm5.4\times10$	$4.1\times10^2\pm2.1\times10$**	$1.7\times10^2\pm6.7\times10$**	ND
	10	$1.3\times10^3\pm3.3\times10$	$8.2\times10^2\pm8.4\times10$*	$1.1\times10^2\pm1.7\times10$**	ND	ND
4,000	0	$4.3\times10^3\pm3.3\times10$	$4.3\times10^3\pm6.7\times10$	$4.3\times10^3\pm8.8\times10$	$4.2\times10^3\pm3.3\times10$	$4.2\times10^3\pm3.3\times10$
	1	$4.2\times10^3\pm1.0\times10^2$	$2.0\times10^3\pm2.6\times10^2$*	$7.0\times10^2\pm4.4\times10$**	$1.1\times10^2\pm1.3\times10$**	ND
	10	$4.2\times10^3\pm1.0\times10$	$9.7\times10^2\pm8.8\times10$**	$1.1\times10^2\pm1.3\times10$**	ND	ND

Units are expressed as copy numbers of poliovirus VP2 genes/0.1 ml. Data are mean±standard error (SE) of triplicate experiments. TCID, tissue culture infective dose; ND, not detected (less than 100 copies/0.1 ml). *$P<0.05$ vs. control, **$P<0.01$ vs. control.

depended mainly on the positive charge applied to the electrode.

Over centuries, humans have been burdened greatly by various infectious diseases caused by water-borne pathogenic microorganisms including infective gastroenteritis, food poisoning, and poliomyelitis (11). Enteroviruses (polioviruses, coxsackieviruses, and echoviruses) are responsible for diseases such as poliomyelitis, herpangina, hand-foot-mouth disease, encephalitis, and meningitis (8). These viruses, which can cause water-borne infections in swimmers are relatively resistant to chemical agents such as hypochlorite (14). Norovirus, recognized as a water-borne agent, is virologically similar to poliovirus in several aspects (30). Recently, severe acute respiratory syndrome (SARS) virus has been suggested to be excreted in urine and feces, and thus can contaminate waste water as a source of infection (10). Such harmful viruses can be removed from tap water and environmental water (well and waste water) by several disinfection methods including boiling, an ancient practice that unfortunately does not affect heat-stable spores and viruses (16). Various chemical agents such as alcohols (ethanol or butanol), hypochlorous acid, iodoform, and formaldehyde can be used to inactivate various microorganisms, but these can pose hazards in themselves. For example, hypochlorous acid reacts with the amino groups of various compounds to generate trihalomethanes, which can be carcinogenic in humans (5). Filtration methods have been used to remove certain bacteria and fungi (29), but most viruses can pass through these filters. Sobsey et al. have developed an electropositive microporous filtration method (28) that can remove hepatitis A virus, but the filter clogs easily and is costly and not durable; unclogging such a fine-pore filter requires tedious pretreatment (27). Moreover, these filtration methods need high water pressure to remove water-suspended viruses. Our electrode is inexpensive, cost is about $1 per disk, and has relatively large pores (10 to 200 μm). Thus, clogging is less of a problem, and water-suspended polioviruses as well as some bacteria could be removed under low water pressure (7). In the present study, we tried only to eliminate polioviruses, using artificially simple conditions. Additional studies may be needed to examine elimination of viruses in muddy or otherwise degraded water.

Surfaces of biologic particles such as bacteria and viruses carry a negative charge corresponding to the zeta potential (12, 13, 31). For example, the average zeta potentials of *Staphylococcus aureus, Escherichia coli, Bacillus subtilis* spores, and *Saccharomyces cerevisiae* are −12, −13, −20, and −7 mV, respectively; the strength of attraction of these bacteria to the electrode correlated with the magnitude of the zeta potential (unpublished data). In this study, the average zeta potential of poliovirus type 2 was −20 mV. Our results strongly suggest that adsorption of polioviruses to the positively-charged carbon felt electrode reflects the total electrical potential between the surface of the virus and the electrode. In conclusion, our method may be applicable to removal of some microorganisms contaminating water, although additional investigations need to be performed under a variety of experimental conditions.

We thank Mr. Taisei Ishioka, Drs. Kunihisa Kozawa (Gunma Prefectural Institute of Public Health and Environmental Science), and Katsuhiko Mushiake, Masahiro Iseki, Daizo Takaoka, Kikuo Takizawa, and Masashi Yasuda (Ecology and Energy Systems Development Center, SANYO Electric, Gunma, Japan) for constructive discussions. We also thank Mr. Yukihisa Takayama (Microtec Co.) for skillful assistance.

References

1) Davis, H.E., Rosinski, M., Morgan, J.R., and Yarmush, M.L. 2004. Charged polymers modulate retrovirus transduction via membrane charge neutralization and virus aggregation. Biophys. J. 86: 1234–1242.

2) Egorova, E.M. 1994. The validity of the Smoluchowski equation in electrophoretic studies of lipid membranes. Electrophoresis **15**: 1125–1131.
3) Feigin, R.D., and Cherry, J.D. 1981. Epidemiology of infectious diseases, p. 98–125. *In* Mortimer, E.A., and Fox, J.P., Jr. (eds), Textbook of pediatric infectious diseases, 4th ed, Elsevier Science Health Science Div., Amsterdam.
4) Goldsmith, A., Edelman, D.A., and Zatuchni, G.I. 1985. Transcutaneous male sterilization. Res. Front. Fertil. Regul. **3**: 1–8.
5) Golfinopoulos, S.K., Nikolaou, A.D., and Lekkas, T.D. 2003. The occurrence of disinfection by-products in the drinking water of Athens, Greece. Environ. Sci. Pollut. Res. **10**: 368–372.
6) Golub, D., Ben-hur, E., Oren, Y., and Soffer, A. 1987. Electroadsorption of bacteria on porous carbon and graphite electrodes. Bioelectrochem. Bioenerg. **17**: 175–182.
7) Kondo, Y., Iseki, M., Takaoka, D., and Takizawa, K. 2003. Highly efficient collection and deactivation of *Bacillus subtilis* spore with a carbon fiber electrode. Bokin Bobai **31**: 113–121 (in Japanese).
8) Koopmans, M., and Duizer, E. 2004. Foodborne viruses: an emerging problem. Int. J. Food Microbiol. **90**: 23–41.
9) Kurtz, J.B., and Lee, T.W. 1987. Astroviruses: human and animal. Ciba Found. Symp. **128**: 92–107.
10) Leung, T.F., Wong, G.W., Hon, K.L., and Fok, T.F. 2003. Severe acute respiratory syndrome (SARS) in children: epidemiology, presentation and management. Paediatr. Respir. Rev. **4**: 334–339.
11) Lipp, E.K., Huq, A., and Colwell, R.R. 2002. Effects of global climate on infectious disease: the cholera model. Clin. Microbiol. Rev. **15**: 757–770.
12) Lytle, D.A., Johnson, C.H., and Rice, E.W. 2002. A systematic comparison of the electrokinetic properties of environmentally important microorganisms in water. Colloids Surf. B: Biointerfaces **24**: 91–101.
13) Mangia, A.H., Teixeira, L.M., Costa, E.S., and Filho, F. 1995. The electrokinetic surface of five enteropathogenic *Escherichia coli* serogroups. Cell Biophys. **26**: 45–55.
14) Masterson, B.F. 1991. Protection of recreational divers against water-borne microbiological hazards. Undersea Biomed. Res. **18**: 197–203.
15) Nishida, T., Kimura, H., Saitoh, M., Shinohara, M., Kato, M., Fukuda, S., Munemura, T., Mikami, T., Kawamoto, A., Akiyama, M., Kato, Y., Nishi, K., Kozawa, K., and Nishio, O. 2003. Detection, quantitation, and phylogenetic analysis of noroviruses in Japanese oysters. Appl. Environ. Microbiol. **69**: 5782–5786.
16) Osburne, M.S., and Sonenshein, A.L. 1976. Behavior of a temperate bacteriophage in differentiating cells of *Bacillus subtilis*. J. Virol. **19**: 26–35.
17) Program for Appropriate Technology in Health PATH. 1983. Immunization: a key to primary health care. Health Technol. Dir. **3**: 1–6.
18) Pruger, B., Eppmann, P., Donath, E., and Gimsa, J. 1997. Measurement of inherent particle properties by dynamic light scattering: introducing electrorotational light scattering. Biophys. J. **72**: 1414–1424.
19) Rab, M.A., Bile, M.K., Mubarik, M.M., Asghar, H., Sami, Z., Siddiqi, S., Dil, A.S., Barzgar, M.A., Chaudhry, M.A., and Burney, M.I. 1997. Water-borne hepatitis E virus epidemic in Islamabad, Pakistan: a common source outbreak traced to the malfunction of a modern water treatment plant. Am. J. Trop. Med. Hyg. **57**: 151–157.
20) Ramia, S. 1985. Transmission of viral infections by the water route: implications for developing countries. Rev. Infect. Dis. **7**: 180–188.
21) Rhame, F.S., Streifel, A.J., Kersey, J.H., Jr., and McGlave, P.B. 1984. Extrinsic risk factors for pneumonia in the patient at high risk of infection. Am. J. Med. **76**: 42–52.
22) Rigonan, A.S., Mann, L., and Chonmaitree, T. 1998. Use of monoclonal antibodies to identify serotypes of enterovirus isolates. J. Clin. Microbiol. **36**: 1877–1881.
23) Schmidt, N.J., and Emmons, R.W. 1995. Diagnostic procedures for viral, rickettsial and chlamydial infections, p. 1–35. *In* Schmidt, N.J., and Emmons, R.W. (eds), General principles of laboratory diagnostic methods for viral, rickettsial and chlamydial infections, 6th ed, American Public Health Association, Washington, D.C.
24) Schmidt, N.J., and Emmons, R.W. 1995. Diagnostic procedures for viral, rickettsial and chlamydial infections, p. 513–579. *In* Grandien, M., Forsgren, M., and Ehrnst, A. (eds), Enteroviruses and reoviruses, 6th ed, American Public Health Association, Washington, D.C.
25) Sharma, S., Sachdeva, P., and Virdi, J.S. 2003. Emerging water-borne pathogens. Appl. Microbiol. **61**: 424–428.
26) Shimizu, Y. 1989. A sanitation system for cup beverage vending machines. Sanyo Techn. Rev. **21**: 91–98 (in Japanese).
27) Smithies, O. 2003. Why the kidney glomerulus does not clog: a gel permeation/diffusion hypothesis of renal function. Proc. Natl. Acad. Sci. U.S.A. **100**: 4108–4113.
28) Sobsey, M.D., Oglesbee, S.E., and Wait, D.A. 1985. Evaluation of methods for concentrating hepatitis A virus from drinking water. Appl. Environ. Microbiol. **50**: 1457–1463.
29) Sundaram, S., Eisenhuth, J., Howard, G., Jr., and Brandwein, H. 2001. Retention of water-borne bacteria by membrane filters. Part I: Bacterial challenge tests on 0.2 and 0.22 micron rated filters. PDA J. Pharm. Sci. Technol. **55**: 65–86.
30) Thornton, A.C., Jennings-Conklin, K.S., and McCormick, M.I. 2004. Noroviruses: agents in outbreaks of acute gastroenteritis. Disaster Manag. Resp. **2**: 4–9.
31) Wilson, W.W., Wade, M.M., Holman, S.C., and Champlin, F.R. 2001. Status of methods for assessing bacterial cell surface charge properties based on zeta potential measurements. J. Microbiol. Methods **43**: 153–164.

JOURNAL OF CLINICAL MICROBIOLOGY, Feb. 2005, p. 657–661 Vol. 43, No. 2
0095-1137/05/$08.00+0 doi:10.1128/JCM.43.2.657–661.2005
Copyright © 2005, American Society for Microbiology. All Rights Reserved.

Seroprevalence of Noroviruses in Swine

Tibor Farkas,[1,2]* Setsuko Nakajima,[3] Masaaki Sugieda,[4] Xiaoyun Deng,[1] Weiming Zhong,[1] and Xi Jiang[1,2]

Division of Infectious Diseases, Cincinnati Children's Hospital Medical Center,[1] and Department of Pediatrics, University of Cincinnati College of Medicine,[2] Cincinnati, Ohio, and Department of Virology, Medical School, Nagoya City University, Aichi,[3] and Shizuoka Prefectural Institute of Public Health and Environmental Science, Shizuoka,[4] Japan

Received 19 March 2004/Returned for modification 21 May 2004/Accepted 8 October 2004

Noroviruses (NVs) are important human pathogens that cause acute gastroenteritis. Genetically related animal enteric NVs have also been described, but there is no evidence of interspecies transmission of NVs. In this study we characterized antibody prevalence among domestic pigs by using recombinant capsid antigens of two human NVs (Norwalk and Hawaii) and one swine NV (SW918) that is genetically related to GII human NVs. Recombinant SW918 capsid protein expressed in baculovirus self-assembled into virus-like particles (VLPs) that were detected by antibodies against GII (Hawaii and Mexico), but not GI (Norwalk and VA115), human NVs. NVs recognize human histo-blood group antigens as receptors, but SW918 VLPs did not bind to human saliva samples with major histo-blood group types. Seventy-eight of 110 (71%) pig serum samples from the United States and 95 of 266 (36%) pig serum samples from Japan possessed antibodies against SW918. Serum samples from pigs in the United States were also tested for antibodies against human NVs; 63% were positive for Norwalk virus (GI) and 52% for Hawaii virus (GII). These results indicate that NV infections are common among domestic pigs; the finding of antigenic relationships between SW918 and human NVs and the detection of antibodies against both GI and GII human NVs in domestic animals highlights the importance of further studies on NV gastroenteritis as a possible zoonotic disease.

Caliciviridae consists of four genera, *Norovirus* (NV), *Sapovirus* (SV), *Lagovirus*, and *Vesivirus* (7), from which NV and SV mainly cause acute gastroenteritis in humans; therefore, these two genera also are called human caliciviruses (HuCVs). Recently several animal enteric CVs genetically closely related to NV or SV have been reported (1, 9, 10, 21, 23). The porcine enteric CV is the only cultivable enteric CV that is closely related to HuCVs, representing a distinct genogroup within SV (9). The bovine enteric CVs (the Jena and Newbury viruses) represent two distinct clusters of genogroup III (GIII) NV (1, 21), while the swine enteric CVs that are closely related to human NVs represent a distinct cluster within genogroup II (22, 23). The discovery of these animal CVs raised the question about CV gastroenteritis as a zoonotic disease.

The epidemiology and prevalence of animal NVs are not well understood. In The Netherlands, 31.6% of pooled stool specimens from veal calf farms and 4.2% of individual stool specimens from dairy cattle were positive for NVs related to the Newbury virus (25). By using an enzyme-linked immunosorbent assay specific for the Jena virus, a study in Germany showed that 9% of the diarrhea stool samples and 99% of the serum samples collected from dairy cows were positive for Jena virus antigens or antibodies, respectively (2). SW918, a prototype strain of swine NVs that shares 64 to 69% amino acid identity with other cluster representatives within GII NVs, was first detected in the cecum contents of healthy pigs in Japan by reverse transcription-PCR (RT-PCR) in 1997 (22). The antigenic identity of SW918 remains unknown due to a lack of reagents for diagnosis. The detection rate of swine NVs in Japan was low (0.35%), and a similar low detection rate (2%) was reported in The Netherlands (26). Recently, Wang et al. reported the detection of swine NVs in 5 of 275 fecal samples collected from six pig farms in the United States and by redesigning their original primers the detection rate improved to 23% (63/275) (27). The role of NVs in causing disease in pigs remains unclear.

In this study we describe the prevalence of antibody against a swine NV (SW918) in pigs in Japan and the United States by an enzyme immune assay (EIA) based on baculovirus-expressed SW918 virus-like particles (VLPs). We also characterized the antigenic identity of SW918 by using type-specific antibodies raised against human NVs. Furthermore, we investigated the prevalence of antibody among pigs against human NVs to address if cross-species transmission of NVs can occur between animals and humans. Although our results did not have the answer, the data presented in this study highlighted the necessity of studying animal NVs in the future.

MATERIALS AND METHODS

Serum and stool samples. A total of 110 serum samples collected from pigs in the United States were tested for antibodies against SW918 and human NVs (Norwalk and Hawaii). Seventy-six of these were collected from Iowa, 2 from Oregon, and 22 from Texas. No other data were available on these samples. Ten serum samples were collected in Kentucky in 2003 in a slaughterhouse from pigs between 6 to 12 months of age. A total of 266 serum samples collected from ~6-month-old pigs between 1997 and 2003 in Shizuoka prefecture in Japan were tested for antibodies against SW918. Thirty-eight of these samples were collected in 1997, 50 in 1998, 100 in 2002, and 78 in 2003.

A total of 104 stool specimens, 100 collected from healthy pigs and 4 from pigs with diarrhea that were less than 3 months old from a farm in Ohio, and 13 intestinal contents collected from the large intestines of pigs between 6 to 12

* Corresponding author. Mailing address: Division of Infectious Diseases, Cincinnati Children's Hospital Medical Center, 3333 Burnet Ave., Cincinnati, OH 45229-3039. Phone: (513) 636-0131. Fax: (513) 636-7655. E-mail: Tibor.Farkas@cchmc.org.

months of age in a slaughterhouse in Kentucky in 2003 were tested for the presence of NVs by RT-PCR and EIA. Stool and serum specimens were stored at −20°C.

Detection of NVs in stool specimens by RT-PCR. RNA was extracted from stool specimens by using the Trizol reagent (Gibco BRL, Gaithersburg, Md.) according to the manufacturer's instructions. Primer set p289H,I-p290H,I,J,K, targeting the RNA polymerase gene, was used to detect NVs in stool specimens (6, 14). These primers produce a 319-bp amplicon for NVs and are also able to detect SVs with a 331-bp product. To amplify the capsid gene of SW918, p455 including the start codon (underlined) of ORF2 and containing an overhang with SpeI and SalI restriction enzyme sites (CCACTAGTCGAC-GGTGTGAATGA AGATGGCGTC) and p457 including the stop codon (underlined) of ORF2 with an overhang containing a NotI site (GAGCGGCCGC-TCAACGAGCCCGCC TGC) have been utilized. RT-PCR was performed as described previously (4). Human stool samples positive for NVs were included in the extraction and RT-PCR as positive controls. For amplification of the capsid cDNA, the extension time was extended to 3 min.

Baculovirus expression of swine NV capsid protein. The original capsid sequence of SW918 was determined by sequencing overlapping PCR products or cDNA clones covering parts of the gene (23). To express the SW918 capsid protein in baculovirus, the entire capsid gene of SW918 was reamplified from the original stool specimen. The identity of the cDNA clone was verified by sequencing of both ends. In order to construct recombinant baculoviruses, the ~1.6-kbp SW918 capsid gene product was gel purified, digested with SalI and NotI, and cloned into SalI/NotI-digested pFastBac1 vector plasmid. Recombinant baculoviruses were generated by using the Bac-To-Bac baculovirus expression system (Gibco BRL, Life Technologies) according to the manufacturer's instructions. Recombinant bacmid DNA was transfected into *Spodoptera frugiperda* (Sf9) cells, clones with high levels of expression were selected, and viral stocks were prepared. For large-scale expression of the SW918 capsid protein, Sf9 cultures were infected with 5 to 10 multiplicity of infection (MOI) recombinant baculoviruses. Cultures were harvested at 4 to 5 days postinfection. Cells were collected by centrifugation at 3,200 rpm for 15 min (Beckman GPR tabletop centrifuge) and freeze-thawed 3 times. Both cell medium and cell lysates were centrifuged at 10,000 × *g* for 30 min to remove cell debris and baculovirus particles. The supernatants were under-layered with 5 ml of 20% sucrose and centrifuged at 27,000 rpm in a SW28 rotor for 2 h at 4°C in a Beckman L90 centrifuge. Pellets were collected and layered onto 10 to 50% discontinuous sucrose gradients. Gradients were run at 100,000 × *g* for 2.5 h, fractionated, and analyzed on sodium dodecyl sulfate (SDS)–10% polyacrylamide gels. Peak fractions, containing the ~60-kDa capsid protein band, were diluted with 4 volumes of phosphate-buffered saline (PBS) and centrifuged at 100,000 × *g* for 2.5 h, and the pellets were resuspended in PBS and stored at −70°C. The protein concentration of VLP preparations was determined by measuring the optical density at 280 nm (OD_{280}) and visually by running aliquots on SDS 10% polyacrylamide gels containing bovine serum albumin standards.

Antibody detection EIA. EIAs were used to measure specific antibodies in serum samples from pigs. Antigens used in the EIAs were as follows: Norwalk (GI/1) from genogroup I and Hawaii (GII/1) and SW918 from genogroup II NV (8, 15, 17, 19). Equal amounts (50 ng/well) of recombinant VLPs were coated and EIAs were performed as described elsewhere (16, 18). Briefly, proteins were coated onto 96-well microtiter plates (Immulon 2HB; Thermolabsystems, Franklin, Mass.) in PBS overnight at 4°C. Wells coated with mock-infected Sf9 cell culture material served as negative controls. After blotting with 5% BLOTTO (Carnation nonfat milk) in PBS, serum samples diluted in 1% BLOTTO–PBS were added and the plates were incubated for 1 h at 37°C. Horseradish peroxidase (HRP)-conjugated rabbit anti-swine immunoglobulin (ICN, Aurora, Ohio) was added at 1:5,000 dilution in 1% BLOTTO–PBS, and the plates were incubated for 1 h at 37°C. Between each step the plates were washed five times with PBS–0.5% Tween 20. TMB substrate (Kirkegaard & Perry Laboratories Inc., Gaithersburg, Md.) was added and the color reaction was developed for 10 min at room temperature. After adding 100 μl of a 1 M H_3PO_4 solution per well, results were read on a microtiter plate reader at OD_{450}. The cutoff point of the test ($OD_{450} > 0.2$) was established as the mean of the OD_{450} readings of the negative control wells plus 2 standard deviations.

Antigen detection EIA. An antigen detection EIA, developed in our laboratory, was used to test if there are shared antigenic epitopes between SW918 and human NVs. It involved hyperimmune guinea pig and rabbit sera obtained by cross-immunization with three GI (C59, Norwalk, and VA115) (5, 17, 19) and five GII (Grimsby, Hawaii, Mexico, VA207, and VA387) (5, 8, 15, 17, 19) human NV capsid proteins, from which all but C59 and VA115 formed VLPs. After finding the antigenic relatedness of SW918 with human NVs, we applied this human NV EIA to screen stool samples of domestic pigs for the presence of antigenically related animal NVs. Briefly, cross-immunized pooled anti-NV rabbit serum and preimmunization rabbit serum were coated on microtiter plates (Immulon 2HB; Thermolabsystems) at 1:2,000 dilution in PBS overnight at 4°C. Stool samples (20%) prepared in PBS were centrifuged at 12,000 rpm in a microcentrifuge for 10 min, and the supernatants were transferred into fresh tubes containing equal volumes of 5% BLOTTO–PBS. Negative swine stool samples seeded with 10 ng and 100 ng/ml of SW918 VLPs were used as positive control. After blotting with 5% BLOTTO–PBS, stool samples (100 μl/well) were added and the plates were incubated for 2 h at 37°C. Cross-immunized pooled anti-NV guinea pig serum was added at 1:3,500 dilution for 1 h followed by HRP-conjugated goat anti-guinea pig immunoglobulin (ICN) at 1:5,000 dilution. Between each step the plates were washed five times with PBS–0.5% Tween 20. TMB substrate (Kirkegaard & Perry Laboratories Inc.) was added and the color reaction was developed for 10 min at room temperature. After adding 100 μl of a 1 M H_3PO_4 solution per well, results were read on a microtiter plate reader at OD_{450}. The cutoff point of the test ($OD_{450} > 0.2$; positive/negative ratio > 5) was originally established for human stool samples (P. W. Huang, unpublished data).

Western blot analysis. SW918 capsid proteins separated by SDS–10% polyacrylamide gel electrophoresis (PAGE) were electro-blotted onto nitrocellulose membranes (Osmonics Nitro Bind; GE Osmonics Labstore, Minnetonka, Minn.). Membranes were blocked with 5% BLOTTO–PBS overnight, stained with first and HRP-labeled secondary antibodies diluted in PBS–0.2% Tween 20 (PBS-T)– 1% BLOTTO. Signals were detected with a ECL detection system (Amersham Biosciences Corp., Piscataway, N.J.) according to the manufacturer's instruction. All wash steps were done by PBS-T.

Saliva binding assays. Saliva samples from healthy human subjects with known ABO, Lewis, and secretor histo-blood types derived from previous studies were used in the saliva binding EIAs to determine if SW918 also recognizes human histo-blood group antigens (HBGAs) (12). Briefly, human saliva samples were diluted to 1:1,000 in PBS (pH 7.4), boiled for 10 min, centrifuged at 10,000 × *g*, and supernatants were coated onto 96-well microtiter plates (Immulon 2HB; Thermolabsystems) overnight at 4°C. Plates were blocked with 5% BLOTTO–PBS and recombinant SW918 VLPs at 1 μg/ml were added. After incubation at 37°C for 1 h, VLP binding was detected by the pooled anti-NV guinea pig hyperimmune serum obtained by cross-immunization and a HRP conjugate as previously described (12). Between each step the plates were washed five times with PBS–0.5% Tween 20. Recombinant capsid proteins from human NVs MOH (GII/5), Norwalk (GI/1), VA207 (GII/9), and VA387 (GII/4) (3, 17, 19), representing different receptor binding patterns of NV, were used as positive controls in the EIAs (3, 12). To test if addition of human or swine stool samples can make a difference in the binding, boiled and clarified stool samples were added with the SW918 VLPs in a final concentration of 1%. Six human stool samples, of which four enhanced the binding of the Hawaii virus VLPs to synthetic oligosaccharides, and 10 pig stool samples were tested on 12 saliva samples representing all the major HBGA types.

EM. Drops of sucrose gradient purified VLPs were adsorbed onto Formvar/carbon 200 mesh copper grids (Electron Microscopy Sciences, Fort Washington, Pa.), stained with 1% ammonium-molybdate, and examined using a Zeiss EM 10 transmission electron microscope (EM).

RESULTS

Baculovirus-expressed SW918 capsid proteins self-assemble into VLPs. VLP formation was first suggested by the fact that the recombinant SW918 capsid proteins concentrated in the middle (fraction 6) of the sucrose gradients (Fig. 1). Direct evidence was obtained by EM examination. VLPs with typical NV morphology were observed in negative-stained EM grids prepared from the peak fractions containing the 60-kDa SW918 capsid proteins (Fig. 2).

SW918 is antigenically related with human NV. SW918 VLPs were detected in the antigen detection EIA by the pooled rabbit and guinea pig polyvalent antibodies produced by cross-immunization with recombinant capsid proteins of multiple human NVs. To further determine the antigenic identity of SW918, Western blot analyses were performed using antibodies raised against individual human NVs. To ensure comparable results, all serum samples, except the pooled serum, were used in a dilution adjusted for their titer against the

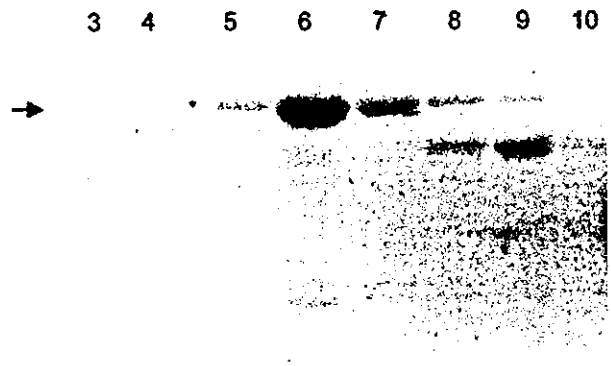

FIG. 1. Electrophoresis of recombinant SW918 VLPs. Discontinuous sucrose gradient (10 to 50%) fractions (f1 to f12) of Sf9 cultures infected with recombinant SW918 baculovirus were collected and analyzed for the presence of SW918 capsid proteins. Equal amounts (5 ul) of fractions (f3 to f10) were separated by SDS-10% PAGE and protein bands were visualized by Coomassie blue staining. The arrow indicates the ~60-kDa full-length capsid protein.

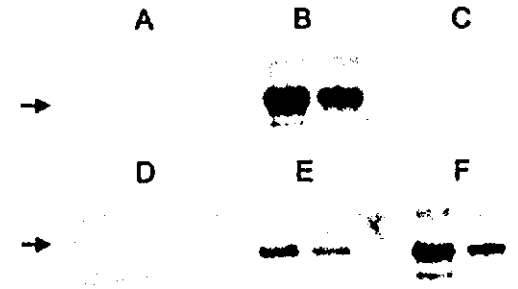

FIG. 3. Western blot immunostaining of SW918 capsid protein. SW918 VLPs (300 and 150 ng) were separated by SDS-10% PAGE, blotted onto nitrocellulose membranes, and stained with anti-NV antibodies raised in guinea pigs. A: preimmunization antibody; B: pooled, cross-immunization antibody (GI + GII); C: anti-Norwalk virus antibody (GI); D: anti-VA115 antibody (GI); E: anti-Mexico virus antibody (GII); F: anti-Hawaii virus antibody (GII). Arrows indicate the ~60-kDa full-length capsid protein.

homologous antigen. Among the four antibodies tested, the SW918 capsid protein reacted with antibodies specific for both GII (Hawaii and Mexico) but neither GI (Norwalk and VA115) NVs (Fig. 3). This result is consistent with the phylogenetic grouping of SW918 belonging to GII of NV.

Search for NVs in swine stools by EIA and RT-PCR. Since the SW918 capsid protein was detected by the cross-immunization sera against human NVs (both rabbit and guinea pig), we screened pig stools for the presence of NVs by using an antigen detection EIA developed for the detection of human NVs in our laboratory (18). The original stool specimen containing the prototype SW918 virus and originally negative pig stool samples seeded with SW918 VLPs gave positive reactions in the test. When stool samples collected from pigs less than 3 months old were tested, 2 of the 104 samples, both collected from healthy pigs, gave OD values significantly higher (0.45 and 1.5) than the cutoff value of the test ($OD_{450} > 0.2$; P/N > 5). However, neither EM nor RT-PCR demonstrated the presence of NV in these stools. We hypothesize that the EIA signals either were nonspecific or that the stool specimens may contain diverse strains missed by the primers originally designed to detect human NVs. None of the 104 stool specimens and 13 intestinal contents collected from pigs were positive in the RT-PCR. Future study to test these stool specimens with additional primers is necessary.

SW918 does not recognize human histo-blood group antigens. Human NVs are known to recognize human HBGAs as receptors. To address the issue of interspecies transmission of NVs, we tested SW918 VLPs for their ability to bind to human HBGAs. Among 52 human saliva samples representing the major ABO, Lewis, and secretor HBGA types tested, none reacted with SW918 VLPs even when higher concentrations of both saliva and SW918 VLPs were used (data not shown). Addition of human or pig stool samples did not promote binding. This result indicates that SW918 does not share the same receptors with the four representative binding patterns of NVs described in our previous studies (12).

FIG. 2. Negatively stained SW918 VLPs. Grids were stained with 1% ammonium-molybdate and examined using a Zeiss EM 10 transmission electron microscope. Arrows indicate VLPs with typical morphology.

High prevalence of antibodies against SW918 was detected in pigs raised in the United States or Japan. Seventy-eight of the 110 (71%) serum samples collected from pigs in the United States reacted with an OD_{450} reading of >0.2 at a dilution of 1:100 and 13% at a dilution of 1:1,000 in the SW918 EIA. The OD ranged from 0.2 to 2.7 with a mean OD of 0.7 for the positive samples at 1:100 dilution (Table 1).

Ninety-five of the 266 (36%) serum samples collected in Japan reacted with an OD_{450} higher than the cutoff value at a dilution of 1:100 and 17% at a dilution of 1:1,000 in the SW918 EIA. Samples collected in 1997 gave the highest detection rates (82% at 1:100 and 39% at 1:1,000) and samples collected in 2002 gave the lowest detection rates (18% at 1:100 and 7% at 1:1,000) (Table 1).

High prevalence of antibodies in pigs was also detected against the prototype Norwalk virus. Surprisingly, 63% of the

TABLE 1. Prevalence of antibodies against SW918 VLPs in pigs raised in Japan or the United States

Location and year	No. of serum samples tested	Prevalence (%) of antibody at serum dilution of:	
		10^{-2}	10^{-3}
Japan			
1997	38	82	39
1998	50	44	20
2002	100	18	7
2003	78	31	14
United States			
Unknown	110	71	13

TABLE 2. Prevalence of antibodies against Hawaii (GII) and Norwalk (GI) VLPs in pigs raised in the United States

Antigen	No. of serum samples tested	Prevalence (%) of antibody at serum dilution of:	
		10^{-2}	10^{-3}
Hawaii	110	52	0
Norwalk	110	63	1

110 pig serum samples collected in the United States reacted with the Norwalk viral antigen at a dilution of 1:100 and 1% at a dilution of 1:1,000, but only 52 and 0% reacted with the Hawaii antigen, respectively (Table 2). The OD values at 1:100 dilution ranged between 0.2 and 0.8 with a mean of 0.37 for Norwalk and between 0.2 and 0.6 with a mean of 0.3 for Hawaii. Since SW918 and Norwalk belong to different genetic groups of NVs and represent different antigenic types, it is unlikely that the observed antibodies against Norwalk virus were induced by SW918-like strains. This possibility also is excluded by the fact that several pigs had high titers of antibodies against SW918 but low titers or no detectable antibodies against Norwalk virus. Fifty-two of the 110 (47%) serum samples were positive for antibodies against all three antigens tested. Three sera were positive only for antibodies against the SW918 antigen and one for antibodies against the Norwalk antigen. All Hawaii antigen-positive serum samples were also positive for SW918.

DISCUSSION

This study was initiated for the characterization of the antigenicity of a swine NV (SW918) that is genetically closely related to GII human NVs. Following the expression of the SW918 capsid proteins in baculovirus, we further demonstrated that SW918 VLPs were antigenically related with human GII NVs, confirming the genetic classification. This result raised several questions related to the origin of the strain and the possibility of cross-species transmission of NVs between animals and humans. Because these questions are important in understanding the epidemiology, immunology, and host range of NVs, we performed further studies to address them.

First we investigated whether SW918 or SW918-like viruses can be detected in pigs raised in the United States. By taking advantage of the cross-reactivity between SW918 and human NVs, we used a well-established human NV antigen detection EIA in an attempt to find antigenically related NVs in pig specimens. We also screened pig stool specimens by RT-PCR with a broadly reactive primer set to increase the chance of finding NVs. However, none of these attempts ended with a conclusive result. Some possible explanations of the negative result are the following: (i) the majority of the samples tested were nondiarrhea stool specimens and the samples came from one pig farm at one time point; (ii) our primers were designed for the detection of human NVs and they might have limitations detecting swine NVs; and (iii) the presence of RT-PCR inhibitors in the pig stools cannot be excluded. Future studies with larger collection of samples particularly of diarrhea stool samples and samples collected from pigs at different ages are necessary and confirmation of the two EIA positive samples by RT-PCR with different primers is a possibility.

Second, we investigated whether SW918 shares common host specificity with human NVs. Recently, human NV infection has been linked to HBGAs, and at least four different receptor recognition patterns have been identified according to the host blood types, including the secretor, ABO, and Lewis types (12). In this study, however, the SW918 VLPs did not bind to HBGAs present in human saliva, indicating it may not be able to target human cells. This result is not unexpected because it is known that most of the HBGAs are species specific, although common epitopes may exist. In our studies to measure the level of human HBGAs in saliva samples and test receptor binding, dried cow milk (BLOTTO) was used as the blocking reagent and we did not observe any interference in the test by the cow milk, indicating that cows do not share HBGAs with humans. This is also in accordance with the report by Hutson et al. (13) in which Norwalk virus that is known to bind to secretor A and O types was able to agglutinate red blood cells from humans and chimpanzees but not from other mammals.

However, we still cannot rule out the possible role of other ligands expressed in the intestine but not present in saliva in NV infection. Also, recent data suggested that stool components may enhance the attachment of NV VLPs to HBGAs (11). In our study, we tested human and swine stool samples for their ability to promote SW918 VLP binding to human saliva samples, but no such effect was observed (data not shown). Although these results do not suggest that SW918 can cause cross-species transmission to humans, the close genetic relationship of this strain to human NVs should alert us to the possible emergence of new strains with wider host ranges by either genomic RNA recombination or mutation during NV replication. In our recent studies mapping the receptor binding domain of NVs, a possible binding pocket on the P2 domain of the capsid has been identified and significant changes of receptor binding patterns of NVs have been observed by site-directed mutagenesis analysis within the pocket region even with a single amino acid change (24). Thus, it seems possible for an animal NV to jump to humans even if it is not native to humans. This is particularly true for strains like SW918 that are genetically close to human strains.

Third, we investigated how frequently SW918 causes infection in pigs. The high antibody prevalence observed in this study clearly indicated that infections of SW918 and/or SW918-like strains are common in pigs in both Japan and the United States. We tried to avoid the possibility of nonspecific reaction of the assays by using highly purified SW918 VLPs. This possibility also could be excluded by the fact that individual pigs revealed different levels of antibodies against the different human and swine NV capsid antigens. The high antibody prevalence is clearly contrary to the low detection rates of swine NVs in previous reports (22, 26) and the failure to detect any in this study by RT-PCR. As described above, multiple factors could result in the low detection rates and future studies about avoiding these factors are necessary.

We finally tested if antibody against human NVs can be detected in animals. Surprisingly, high levels of antibody prevalence against human NVs in pigs were detected. Even more interestingly, we observed a higher level of antibody prevalence

against a GI than a GII human NV. SW918 belongs to GII and we showed that it is antigenically distant from GI NVs, so the antibodies detected against Norwalk did not likely result from a cross-reaction with SW918 or SW918-like strains. These results also indicate that, as in humans, wide genetic and antigenic types of NVs may cocirculate in animals.

We realize that this study has limitations. For example, the antibody levels in pigs were not as high as the antibody levels against human NVs observed in human populations (20). One possibility is that most of the antibodies detected in this study probably resulted from heterologous responses against different antigenic types. Future studies with more recombinant capsid proteins representing different antigenic types in the EIAs may be necessary. Furthermore, the antibody detection experiments were performed in separate laboratories in the United States and Japan because of U.S. Department of Agriculture regulations for importing samples of animal origin. Although standard protocols were used in both laboratories, not all reagents were shared and variations of the results between the two laboratories remain possible. In conclusion, although this study did not provide the final answer of whether NVs can cause cross-species transmission, the findings of the antigenic relationship of SW918 with human NVs and the high seroprevalence against both animal and human NVs in pigs are significant. Future studies to look more closely on NV activities in the animal kingdom are necessary.

ACKNOWLEDGMENTS

We thank Kim Green for sharing the recombinant capsid protein of Hawaii virus and Irene Hofmann for helping with the EM.

This study was supported by the Cincinnati Children's Hospital Research Foundation Trustee grant and the National Institutes of Health (R01 AI37093).

REFERENCES

1. **Dastjerdi, A. M., J. Green, C. I. Gallimore, D. W. Brown, and J. C. Bridger.** 1999. The bovine Newbury agent-2 is genetically more closely related to human SRSVs than to animal caliciviruses. Virology **254**:1–5.
2. **Deng, Y., C. A. Batten, B. L. Liu, P. R. Lambden, M. Elschner, H. Gunther, P. Otto, P. Schnurch, W. Eichhorn, W. Herbst, and I. N. Clarke.** 2003. Studies of epidemiology and seroprevalence of bovine noroviruses in Germany. J. Clin. Microbiol. **41**:2300–2305.
3. **Farkas, T., T. Berke, G. Reuter, G. Szucs, D. O. Matson, and X. Jiang.** 2002. Molecular detection and sequence analysis of human caliciviruses from acute gastroenteritis outbreaks in Hungary. J. Med. Virol. **67**:567–573.
4. **Farkas, T., X. Jiang, M. L. Guerrero, W. Zhong, N. Wilton, T. Berke, D. O. Matson, L. K. Pickering, and G. Ruiz-Palacios.** 2000. Prevalence and genetic diversity of human caliciviruses (HuCVs) in Mexican children. J. Med. Virol. **62**:217–223.
5. **Farkas, T., S. A. Thornton, N. Wilton, W. Zhong, M. Altaye, and X. Jiang.** 2003. Homologous versus heterologous immune responses to Norwalk-like viruses among crew members after acute gastroenteritis outbreaks on 2 US Navy vessels. J. Infect. Dis. **187**:187–193.
6. **Farkas, T., W. Zhong, Y. Jing, P. Huang, S. Espinosa, N. Martinez, A. L. Morrow, G. Ruiz-Palacios, L. K. Pickering, and X. Jiang.** 2004. Genetic diversity among sapoviruses. Arch. Virol. **149**:1309–1323.
7. **Green, K. Y., T. Ando, M. S. Balayan, T. Berke, I. N. Clarke, M. K. Estes, D. O. Matson, S. Nakata, J. D. Neill, M. J. Studdert, and H. J. Thiel.** 2000. Taxonomy of the caliciviruses. J. Infect. Dis. **181**(Suppl. 2):S322–S330.
8. **Green, K. Y., A. Z. Kapikian, J. Valdesuso, S. Sosnovtsev, J. J. Treanor, and J. F. Lew.** 1997. Expression and self-assembly of recombinant capsid protein from the antigenically distinct Hawaii human calicivirus. J. Clin. Microbiol. **35**:1909–1914.
9. **Guo, M., K. O. Chang, M. E. Hardy, Q. Zhang, A. V. Parwani, and L. J. Saif.** 1999. Molecular characterization of a porcine enteric calicivirus genetically related to Sapporo-like human caliciviruses. J. Virol. **73**:9625–9631.
10. **Guo, M., J. F. Evermann, and L. J. Saif.** 2001. Detection and molecular characterization of cultivable caliciviruses from clinically normal mink and enteric caliciviruses associated with diarrhea in mink. Arch. Virol. **146**:479–493.
11. **Harrington, P. R., J. Vinje, C. L. Moe, and R. S. Baric.** 2004. Norovirus capture with histo-blood group antigens reveals novel virus-ligand interactions. J. Virol. **78**:3035–3045.
12. **Huang, P., T. Farkas, S. Marionneau, W. Zhong, N. Ruvoen-Clouet, A. L. Morrow, M. Altaye, L. K. Pickering, D. S. Newburg, J. LePendu, and X. Jiang.** 2003. Noroviruses bind to human ABO, Lewis, and secretor histo-blood group antigens: identification of 4 distinct strain-specific patterns. J. Infect. Dis. **188**:19–31.
13. **Hutson, A. M., R. L. Atmar, D. M. Marcus, and M. K. Estes.** 2003. Norwalk virus-like particle hemagglutination by binding to H histo-blood group antigens. J. Virol. **77**:405–415.
14. **Jiang, X., P. W. Huang, W. M. Zhong, T. Farkas, D. W. Cubitt, and D. O. Matson.** 1999. Design and evaluation of a primer pair that detects both Norwalk- and Sapporo-like caliciviruses by RT-PCR. J. Virol. Methods **83**: 145–154.
15. **Jiang, X., D. O. Matson, G. M. Ruiz-Palacios, J. Hu, J. Treanor, and L. K. Pickering.** 1995. Expression, self-assembly, and antigenicity of a snow mountain agent-like calicivirus capsid protein. J. Clin. Microbiol. **33**:1452–1455.
16. **Jiang, X., J. Wang, and M. K. Estes.** 1995. Characterization of SRSVs using RT-PCR and a new antigen ELISA. Arch. Virol. **140**:363–374.
17. **Jiang, X., M. Wang, D. Y. Graham, and M. K. Estes.** 1992. Expression, self-assembly, and antigenicity of the Norwalk virus capsid protein. J. Virol. **66**:6527–6532.
18. **Jiang, X., N. Wilton, W. M. Zhong, T. Farkas, P. W. Huang, E. Barrett, M. Guerrero, G. Ruiz-Palacios, K. Y. Green, J. Green, A. D. Hale, M. K. Estes, L. K. Pickering, and D. O. Matson.** 2000. Diagnosis of human caliciviruses by use of enzyme immunoassays. J. Infect. Dis. **181**(Suppl. 2):S349–S359.
19. **Jiang, X., W. M. Zhong, T. Farkas, P. W. Huang, N. Wilton, E. Barrett, D. Fulton, R. Morrow, and D. O. Matson.** 2002. Baculovirus expression and antigenic characterization of the capsid proteins of three Norwalk-like viruses. Arch. Virol. **147**:119–130.
20. **Jing, Y., Y. Qian, Y. Huo, L. P. Wang, and X. Jiang.** 2000. Seroprevalence against Norwalk-like human caliciviruses in Beijing, China. J. Med. Virol. **60**:97–101.
21. **Liu, B. L., P. R. Lambden, H. Gunther, P. Otto, M. Elschner, and I. N. Clarke.** 1999. Molecular characterization of a bovine enteric calicivirus: relationship to the Norwalk-like viruses. J. Virol. **73**:819–825.
22. **Sugieda, M., H. Nagaoka, Y. Kakishima, T. Ohshita, S. Nakamura, and S. Nakajima.** 1998. Detection of Norwalk-like virus genes in the caecum contents of pigs. Arch. Virol. **143**:1215–1221.
23. **Sugieda, M., and S. Nakajima.** 2002. Viruses detected in the caecum contents of healthy pigs representing a new genetic cluster in genogroup II of the genus "Norwalk-like viruses." Virus Res. **87**:165–172.
24. **Tan, M., P. Huang, J. Meller, W. Zhong, T. Farkas, and X. Jiang.** 2003. Mutations within the P2 domain of norovirus capsid affect binding to human histo-blood group antigens: evidence for a binding pocket. J. Virol. **77**: 12562–12571.
25. **van der Poel, W. H., R. van der Heide, F. Verschoor, H. Gelderblom, J. Vinje, and M. P. Koopmans.** 2003. Epidemiology of Norwalk-like virus infections in cattle in The Netherlands. Vet. Microbiol. **92**:297–309.
26. **van der Poel, W. H., J. Vinje, R. van der Heide, M. I. Herrera, A. Vivo, and M. P. Koopmans.** 2000. Norwalk-like calicivirus genes in farm animals. Emerg. Infect. Dis. **6**:36–41.
27. **Wang, Q. H., S. Cheetham, M. Souza, M. G. Han, W. Zhang, J. Funk, and L. J. Saif.** 2004. Prevalence and molecular characterization of porcine noroviruses and sapoviruses. W38-9. 23rd Annu. Meet. Am. Soc. Virol., 10 to 14 July 2004. McGill University, Montreal, Quebec, Canada.

JOURNAL OF VIROLOGY, Apr. 2004, p. 3889–3896 Vol. 78, No. 8
0022-538X/04/$08.00+0 DOI: 10.1128/JVI.78.8.3889–3896.2004
Copyright © 2004, American Society for Microbiology. All Rights Reserved.

Poly(A)- and Primer-Independent RNA Polymerase of *Norovirus*

Shuetsu Fukushi,[1]† Shigeyuki Kojima,[1] Reiko Takai,[1] Fuminori B. Hoshino,[1] Tomoichiro Oka,[2] Naokazu Takeda,[2] Kazuhiko Katayama,[2] and Tsutomu Kageyama[1]*

R&D Center, BioMedical Laboratories, Kawagoe, Saitama 350-1101,[1] and Department of Virology II, National Institute of Infectious Diseases, Musashi-Murayama, Tokyo 208-0011,[2] Japan

Received 27 August 2003/Accepted 27 December 2003

Replication of positive-strand caliciviruses is mediated by a virus-encoded RNA-dependent RNA polymerase (RdRp). To study the replication of *Norovirus* (NV), a member of the family *Caliciviridae*, we used a recombinant baculovirus system to express an enzymatically active RdRp protein from the 3D region of the NV genome and defined conditions for optimum enzymatic activity. Using an RNA template from the NV 3′ genomic region, we observed similar levels of enzymatic activity in assays with and without a poly(A) tail. RdRp activity was not significantly affected by the addition of an RNA primer to the reaction mixture. Thus, the NV RdRp exhibited primer- and poly(A)-independent RNA polymerase activity. While the RdRp inhibitor phosphonoacetic acid inhibited NV RdRp activity, another gliotoxin did not. The active recombinant NV RdRp will be of benefit to studies of NV replication and will facilitate the development of specific inhibitors of NV proliferation.

Norovirus (NV), a member of the family *Caliciviridae*, is the leading cause of epidemic acute, nonbacterial gastroenteritis. NV infection causes nausea, vomiting, low-grade fever, and diarrhea, which can be severe in infants and young children. For these reasons, it is a major public health concern (7). An effective vaccine or other therapeutic agent would be valuable for preventing the significant morbidity and potential mortality associated with NV infections. However, the lack of an efficient culture system has hampered the biochemical characterization of the NV proteins, and thus far, molecular biological techniques have been the most useful tools for the study of NV.

The NV virion contains a polyadenylated plus-strand RNA genome of ~7.7 kb (11, 15). The structures of the full-length genome, phylogenetic trees, and genetic recombination among distinct genogroups have been analyzed in detail (13). Based on sequence similarities with other single-stranded RNA viruses, the NV open reading frame 1 (ORF1) is predicted to encode a large polyprotein that is cleaved into several viral proteins, including NTPase, proteinase, and RNA-dependent RNA polymerase (RdRp) (11, 15).

The RdRp encoded by the 3D region has a conserved amino acid motif, glycine-aspartic acid-aspartic acid (GDD), which is found in the active site of many viral RdRps (14), and thus might have an important role in NV replication. As in other positive-strand RNA viruses (2), NV genomic RNA likely acts as a template for the synthesis of minus-strand RNA. The minus-strand RNA then, in turn, serves as a template for the synthesis of progeny genomic plus-strand RNA molecules. Thus, RdRp is central to the synthesis of both plus- and minus-strand RNA molecules. Among the *Caliciviridae*, *Rabbit hemorrhagic disease virus* (RHDV) and *Feline calicivirus* (FCV) express an enzymatically active RdRp protein (27, 28). However, caliciviruses that infect humans have not been examined for RdRp activity.

The aims of this study were to develop a cell-free system that permits the identification of RdRp activity in vitro and to characterize the biochemical properties of RdRp in NV replication. We expressed the RdRp protein from the 3D region of the NV genome with a baculovirus vector and then tested the activity of the purified protein.

MATERIALS AND METHODS

Construction of plasmids. The primer sequences used for plasmid construction are listed in Table 1.

To obtain a cDNA fragment corresponding to the full-length genome of the NV genogroup 2 strain U201, we used primers U201LV1S-BglII and TX30SXN to amplify viral RNA extracted from a stool specimen (U201) (13). RNA extraction, reverse transcription, and PCR were performed as previously described (13). The 3D region was amplified from the full-length cDNA of strain U201 with the primers EagI-3D and 3D-EcoRI, digested with EagI and EcoRI, and cloned into the EagI-EcoRI site of the pVL1392 vector (BD Bioscience, San Jose, Calif.) to obtain pVLwt3D (Fig. 1).

The plasmid pVLwt3D was used as a template for mutagenesis, and DNA oligonucleotide primers 3D-GAA-F, 3D-GAA-R, 3D-GAD-F, and 3D-GAD-R were used to introduce amino acid substitutions at the conserved GDD motif. To obtain a mutant RdRp containing an amino acid change of the GDD motif to GAA, we amplified the 5′ and 3′ halves of the mutant 3D region by using primer set 3D-GAA-R and EagI-3D or 3D-GAA-F and 3D-EcoRI, respectively. Since the resulting two cDNA fragments partially overlapped each other, they were mixed, denatured, annealed, and filled in with Tbr EXT DNA polymerase (Fynzyme, Espoo, Finland) to obtain the full-length construct with a mutant 3D region. The resulting products were digested with EagI and EcoRI and ligated into the pVL1392 vector to form the plasmid pVLm3D(GAA) (Fig. 1).

We amplified two additional cDNA fragments. To obtain another mutant RdRp that changes the GDD motif to GAD, we amplified the 5′ or 3′ half of the mutant 3D region by using primer set 3D-GAD-R and EagI-3D or 3D-GAD-F and 3D-EcoRI with the same strategy as that used for the construction of plasmid pVLm3D(GAA). To obtain the full-length 3D construct with a GAD mutant, the resulting two cDNA fragments were mixed, denatured, annealed, and filled in with Tbr EXT DNA polymerase. The resulting products were digested with EagI and EcoRI and ligated into the pVL1392 vector to form the plasmid pVLm3D(GAD) (Fig. 1). Finally, the 3B region of the NV genome was

* Corresponding author. Mailing address: R&D Center, BioMedical Laboratories, Matoba 1361-1, Kawagoe, Saitama 350-1101, Japan. Phone: (81)49-232-0440. Fax: (81)49-232-5480. E-mail: tkage@alk.co.jp.

† Present address: Department of Virology I, National Institute of Infectious Diseases, Tokyo 208-0011, Japan.

TABLE 1. Sequences of DNA primers used for plasmid construction

Primer	Polarity	Sequence[a] (5′→3′)
U201LV1S-BglII	+	GAagatctTCGTGAATGAAGATGGCGTCTAACGAC
TX30SXN	−	GACTAGTTCTAGATCGCGAGCGGCCGCCCTTTTTTTTTTTTTTTTTTTTTTTTTTTT
EagI-3D	+	TTTcggccgATGGGAGGTGACGACAAGGGCACCTAT
3D-EcoRI	−	AAAgaattcTTATTATTCGACGCCATCTTCATTCACAAA
3D-GAA-F	+	TTCTATGGTG CTGCTGAGATTGTA
3D-GAA-R	−	CTCA GCAGCACCATAGAAAGAGTA
3D-GAD-F	+	TTCTATGGTG CTGATGAGATTGTA
3D-GAD-R	−	CTCATCA GCACCATAGAAAGAGTA
BamH-3B	+	CGCggatccATGGGAAAGAAAGGCAAGAACAAGTCC
3B-Xba	−	TGCtctagaTTATTATTCAAAATCTATCCTCTCATTGTA
KpnT7ORF3	+	CGGggtaccTAATACGACTCACTATAGGGAAGGATTCAATAATGGCTGGAG
201pAMS	−	TACGGCATGCacgcgtTTTTTTTTTTTTTTTTTTTTTTTTTTTTTTTTTTTTAAAAGATTCTAAATCAAATT
T7S608	+	TTATAATACGACTCACTATAGGACAGCTTTTGTCACTCCACCATC
201ASdelA-Xba	−	GtctagaAAAGATTCTAAATCAAATTTAGG

[a] Restriction sites used for cloning are represented by lowercase letters. The underlined nucleotides were changed to introduce amino acid substitutions at the conserved GDD motif.

amplified, using primers BamH-3B and 3B-Xba. The resulting cDNA was digested with BamHI and XbaI and cloned into the BamHI-XbaI site of the pVL1393 vector (BD Bioscience) to obtain pVL3B (Fig. 1).

A series of plasmids (i.e., pMT-ORF3pA, pUC608-pA, and pUC608delA) was used for in vitro transcription to prepare the RNA templates or RNA size markers for the analysis of RdRp products. These were constructed by PCR with the oligonucleotide primers described below. For the plasmid pMT-ORF3pA, primers KpnT7ORF3 and 201pAMS were used with the full-length cDNA template of U201 to amplify a cDNA fragment from ORF3 to the poly(A) region under the T7 promoter sequence. The resulting product was digested with KpnI and MluI and then cloned into the KpnI and MluI sites of the pMT1 vector (kindly provided by M. Tatsumi, National Institute of Infectious Diseases, Tokyo, Japan). Primers T7S608, which contained the T7 promoter, and 201pAMS were used with template plasmid pMT-ORF3pA to amplify a cDNA fragment corresponding to the 3′-terminal 232 nucleotides of the NV genome. The amplified product was ligated to the pT7Blue vector (Takara Bio, Shiga, Japan) to obtain pT7608-pA. The HindIII-EcoRI fragment of the cDNA was inserted into the HindIII-EcoRI site of the pUC119 vector and the plasmid was designated pUC608-pA. Primers T7S608 and 201AsdelA-Xba were used with template plasmid pMT-ORF3pA to amplify a cDNA fragment that corresponded to plasmid pUC608-pA except for a deletion of the poly(A) sequence. The PCR product was inserted into the pT7Blue vector to obtain pT7608delA. By the same strategy, the HindIII-EcoRI fragment of the cDNA was cloned into the pUC119 vector to obtain pUC608delA.

Preparation of RNA. The oligo$(U)_{15}$ RNA primer was purchased from Takara Bio. The RNA dimer UpU was purchased from Sigma (Tokyo, Japan). ORF3-pA, 608-pA, and 608-delA RNAs were transcribed in vitro by T7 RNA polymerase (Promega, Tokyo, Japan) from the templates MluI-digested pMT-ORF3pA, MluI-digested pUC608-pA, and XbaI-digested pUC608delA, respectively. The RNAs were purified, and their integrity was verified as described previously (6).

Expression and purification of RdRp protein. The procedures for generating recombinant baculoviruses and for subsequent large-scale production of the proteins were adapted from the work of Li et al. (16). Briefly, transfer plasmid pVLwt3D, pVLm3D (GAA), pVLm3D (GAD), or pVL3B was cotransfected into insect SF9 cells with linearized BaculoGold DNA (BD Bioscience) to obtain recombinant baculovirus BVwt3D, BVm3D(GAA), BVm3D(GAD), or BV3B, respectively. Insect Tn5 cells were infected with these recombinant baculoviruses for the large-scale expression of recombinant RdRp proteins. After 4 days of incubation at 27°C, cells were harvested, collected by centrifugation, and washed twice with phosphate-buffered saline.

The cell pellet was resuspended in ice-cold cell lysis buffer (20 mM Tris-HCl [pH 7.5], 1.0 mM EDTA, 10 mM dithiothreitol [DTT], 2% Triton X-100, 500 mM NaCl, 10 mM $MgCl_2$, 50% glycerol, and EDTA-free protease inhibitors)

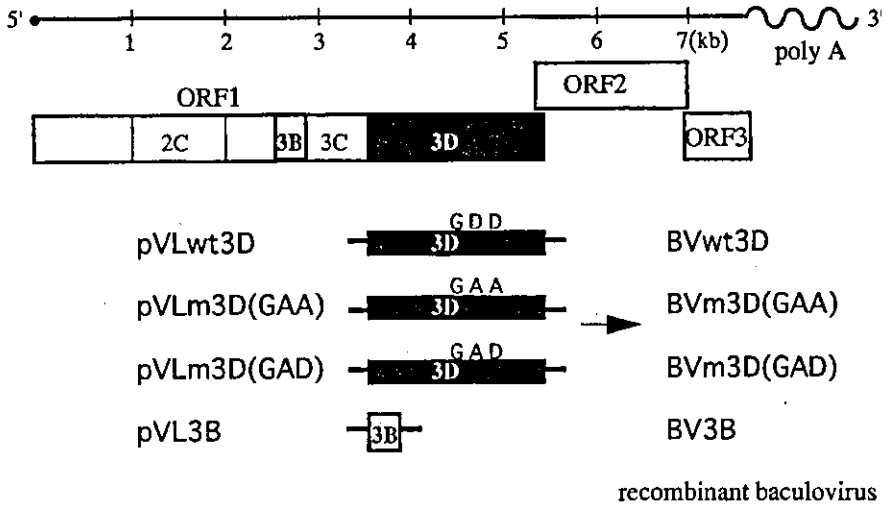

FIG. 1. Expression constructs for RdRp proteins. The genome structure of NV is shown to scale. The 3D region with the wild-type GDD motif (wt3D) and with amino acid substitutions of GDD to GAA [m3D(GAA)] or GAD [m3D(GAD)] and the 3B region of the NV cDNA were inserted into baculovirus transfer vectors to construct recombinant baculoviruses.

(Roche Diagnostics, Tokyo, Japan). The extract was sonicated, cleared of debris by centrifugation at 15,000 × *g* for 30 min, dialyzed against SP buffer (25 mM morpholineethanesulfonic acid [pH 6.4], 1.0 mM EDTA, and 1% Triton X-100), and applied to a HiTrap SP column (Amersham Biosciences) that was pre-equilibrated with SP buffer. Bound proteins were eluted by a linear gradient of 0 to 1.0 M NaCl in SP buffer and were analyzed by sodium dodecyl sulfate (SDS)-polyacrylamide gel electrophoresis and Coomassie blue staining. The RdRp protein was eluted with 320 to 550 mM NaCl, dialyzed against RdRp sample buffer (20 mM Tris-HCl [pH 7.7], 1.0 mM EDTA, 100 mM NaCl, 10 mM DTT, 2% Triton X-100, and 50% glycerol), and tested for RdRp activity. The fractions containing active RdRp protein were combined, dialyzed against Q buffer (20 mM Tris-HCl [pH 7.7], 1.0 mM EDTA, and 1% Triton X-100), and applied to a HiTrap Q column (Amersham Biosciences) that was pre-equilibrated with Q buffer. Bound proteins were eluted with a linear gradient of 0 to 1.0 M NaCl in Q buffer and were analyzed by SDS-polyacrylamide gel electrophoresis and Coomassie blue staining. RdRp fractions eluted at ~520 mM NaCl. They were combined, dialyzed against RdRp sample buffer, and examined for RdRp activity.

RdRp and terminal nucleotidyl transferase (TNTase) assays. The RdRp reaction was performed in a 15-μl volume with 375 ng of RdRp protein and 5.0 pmol of in vitro-transcribed ORF3-pA RNA, 608-polyA RNA, or 608-delA RNA in a reaction buffer containing, unless otherwise specified, 20 mM Tris-HCl (pH 6.8), 2.0 mM $MnCl_2$, 100 mM NaCl, 20 mM DTT, 20 U of RNase inhibitor (Promega), 50 μg of actinomycin D/ml, 250 μM GTP, 125 μM ATP, 125 μM CTP, 5.0 μM UTP, and 4.0 μCi of [^{33}P]UTP (>2,500 Ci/mmol) (Amersham Biosciences).

Nuclease digestion was performed as described by Ishii et al. (10). TNTase assays were performed in the same buffer with specified nucleoside triphosphates. RdRp and TNTase reactions were done at 30°C for 90 min and stopped by the addition of 60 μl of a stop solution (10 mM Tris-HCl [pH 7.5], 10 mM EDTA, 100 mM NaCl). The RNA products were extracted with TRISOL LS reagent (Invitrogen, Tokyo, Japan) and precipitated with isopropanol. Products were dissolved with RNA sample buffer containing 80% formamide, 1 mM EDTA, and 0.1% bromophenol blue. After heat denaturation, the RNA products were separated in 6.0 or 10.0% polyacrylamide gels in 8.0 M urea. Radiolabeled RNA products were analyzed with the BAS 1000 system (Fuji Film, Tokyo, Japan).

For the examination of polymerase inhibitors, phosphonoacetic acid (PAA) and gliotoxin were purchased from Sigma. These materials were dissolved in H_2O, and then increasing amounts (25, 100, and 250 μM) of the inhibitors were mixed with the RdRp reaction buffer.

RESULTS

Expression and purification of enzymatically active RdRp proteins. In FCV, a member of the family *Caliciviridae*, the proteinase-polymerase precursor (3CD) rather than the 3D region itself is highly active, which may be attributed to inefficient proteolytic processing of the linker domain of 3CD (25, 28). Since efficient proteolytic processing of the NV polyprotein into 3D is observed in both *Escherichia coli* and mammalian cell expression systems (17, 24), we cloned and expressed the 3D region itself to study the biochemical properties of NV RdRp (Fig. 1). A recombinant baculovirus system was used to express NV RdRp. Soluble lysates of infected cells were separated by cation-exchange chromatography (Fig. 2A), and fractions were examined for RdRp activity.

Several investigators have shown that viral RdRps have primer-dependent RNA polymerase activities with homopolymeric RNA templates (5, 10, 28). To clarify the molecular mechanism of NV replication, it is more important to test the activity with the viral RNA template than with the homopolymeric RNA template. In this study, we examined the NV RdRp activity with synthetic RNA templates that corresponded to the 3′-terminal region of the NV genome. We believe that our strategy for measuring NV RdRp activity better replicates the production of minus-strand RNA from plus-strand genomic RNA.

The template ORF3-pA RNA (Fig. 2B) was incubated with RdRp fractions in the presence of [^{33}P]UTP and cold ribonucleotide triphosphates. Radiolabeled reaction products of RdRp assays were analyzed in denaturing polyacrylamide gels. [^{33}P]UTP was incorporated in fractions from BVwt3D-infected cell lysates that eluted at 320 to 550 mM NaCl (Fig. 2C).

We next examined whether the nucleotide length of the RNA product obtained by the RdRp assay was the same as that obtained with the template ORF3-pA RNA. As a size marker, we prepared T7 RNA polymerase-labeled RNA transcribed from MluI-digested plasmid pMT-ORF3pA (Fig. 2C, lane 1). The template RNA for the RdRp assays was also transcribed from the same starting material by T7 RNA polymerase (see Materials and Methods). The lengths of the RNA products from the RdRp assays were identical to that of the template, indicating that the RNA products of the RdRp reaction were transcripts of the template RNA. On the other hand, incorporation was at background levels in the lysates of negative control cells infected with BVm3D(GAA) and BV3Dm(GAD), which carried amino acid substitutions at a GDD motif (Fig. 2C).

To analyze the activity of the wild-type RdRp protein in detail, we collected the active RdRp fractions from cation-exchange chromatography and subsequent anion-exchange chromatography steps (Fig. 2A). Purified RdRp protein was used for further analyses.

Characterization of RdRp activity. We next examined the effects of pH and divalent cation concentrations, including $MgCl_2$, $MnCl_2$, and $CaCl_2$, on NV RdRp activity. ORF3-pA RNA synthesized in vitro was used as a template. Since the requirements of divalent cations are different for primer-dependent and primer-independent synthesis (21), the oligonucleotide primer was not used in the reaction. RdRp activity was markedly increased in the presence of 2.0 mM Mn^{2+}. A slight increase was detected with increased concentrations of Mg^{2+}, although to a much lesser extent than with Mn^{2+}. No increase was seen with Ca^{2+} (Fig. 3A). The RdRp activity was found to be optimal at pHs 6.8 to 7.5 (data not shown). Based on these results, we used pH 6.8 and 2.0 mM Mn^{2+} for further studies of NV RdRp activity.

We also examined the possibility that the synthesis was due to a DNA-dependent RNA polymerase in the extracts of insect Tn5 cells. To do this, we added actinomycin D to the reaction mixtures. Actinomycin D forms a complex with DNA and interferes with RNA synthesis. The production of labeled RNA with RdRp assays was not inhibited in the presence of various amounts of the inhibitor (Fig. 3B), indicating that the labeled RNA had not originated from the action of a DNA-dependent RNA polymerase.

Characterization of RdRp products. Hepatitis C virus (HCV) RdRp expressed in recombinant baculovirus systems shows TNTase activity (20). TNTase activity might confound the interpretation of the actual properties of RdRp. Since TNTase labels the 3′ ends of RNA, the RNA product in our RdRp assays could result from the addition of [^{33}P]UTP to the 3′ end of the template RNA by TNTase. To examine this possibility, we performed TNTase assays without cold ATP, CTP, and GTP. The template 608-pA RNA contained the NV

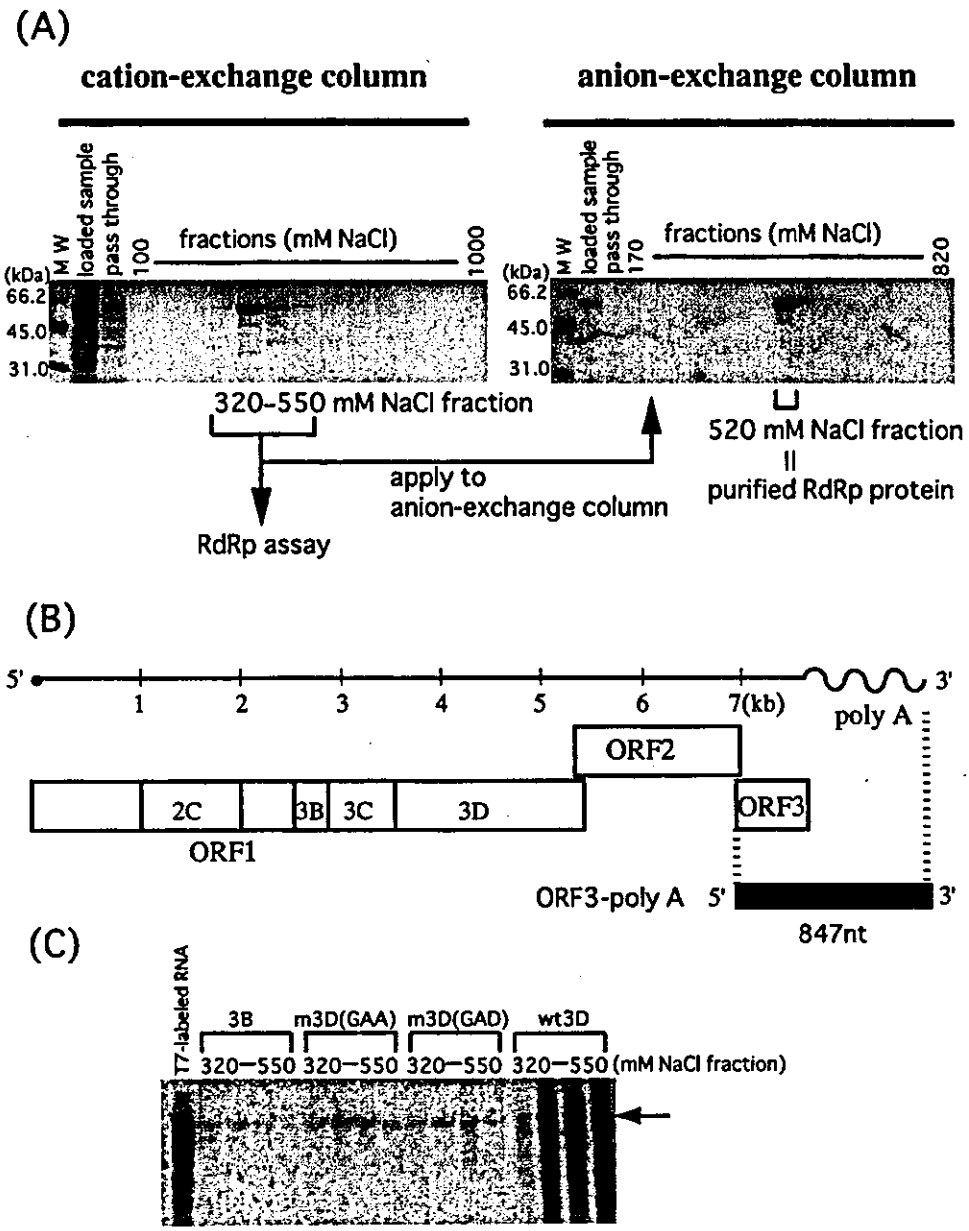

FIG. 2. Purification and enzymatic activity of NV RdRp. (A) Eluted proteins from a HiTrap SP (cation exchange) column (left) and a HiTrap Q (anion exchange) column (right) were separated by SDS-polyacrylamide gel electrophoresis and visualized by Coomassie blue staining. The portions of fractions containing RdRp protein eluted by 320 to 550 mM NaCl in SP buffer from the cation-exchange column were used to examine enzymatic activity. The fractions with active RdRp from the cation-exchange column were then subjected to further purification in the anion-exchange column. (B) Genome structure of NV shown to scale. The RNA template used for RdRp assays is represented by a black bar. (C) RdRp reaction with the fractions from a cation-exchange column. At the same time, m3D(GAA) and m3D(GAD), which had substitutions in the GDD motif to GAA and GAD, respectively, and 3B protein as a negative control were separated in cation-exchange columns, and the eluted fractions were subjected to an RdRp assay using the same strategy as that used for the wild-type protein (wt3D). RNA products were separated in a denaturing polyacrylamide gel, analyzed by the BAS1000 system, and presented together with [^{33}P]-incorporated molecular size markers transcribed by T7 RNA polymerase from MluI-digested pMT-ORF3pA (T7-labeled RNA).

3'-terminal region and 30 nucleotides of poly(A) sequence (Fig. 4). [^{33}P]-labeled RNA products were not detected in the TNTase assays in the presence of [^{33}P]UTP only or [^{33}P]UTP plus cold UTP, without any other NTPs (Fig. 4, lanes 2 and 3). The RdRp protein did not display any activity that added UTP to the 3' end of the template RNA. Therefore, the labeled RNA product was not the result of TNTase activity.

We next determined whether the products synthesized from the NV RNA template were single or double stranded. Double-stranded RNA would indicate that cRNA is synthesized

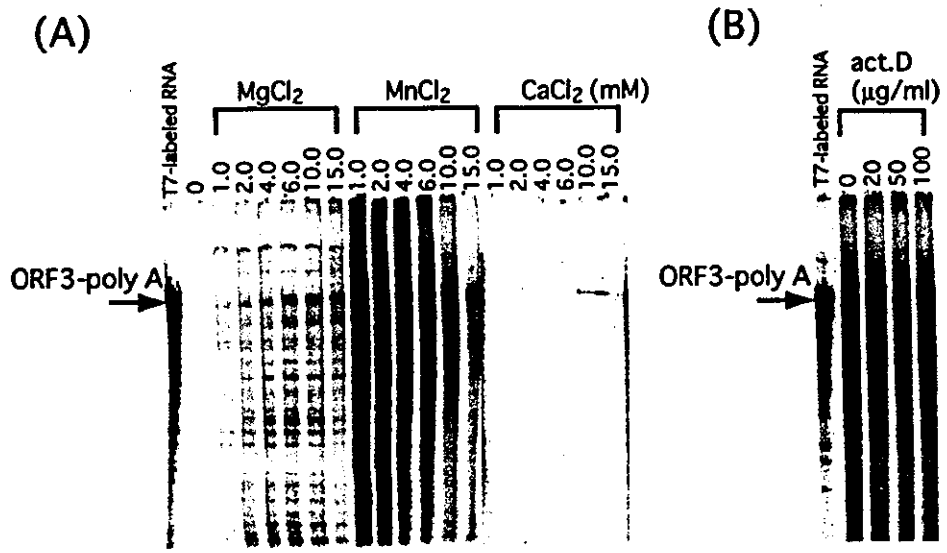

FIG. 3. Optimization of RdRp assay conditions and effects of actinomycin D on enzymatic activity. The RNA template used for RdRp assays is shown in Fig. 2B. (A) Divalent cation optimization. (B) Effects of increasing amounts of actinomycin D on enzymatic activity. RNA products were analyzed using methods similar to those described for Fig. 2.

from the template RNA by RdRp. Since S1 nuclease catalyzes the specific degradation of single-stranded RNA to mononucleotides, the RdRp product was incubated with S1 nuclease. The 608-pA RNA containing the 3′-terminal region of the NV genome and the poly(A) sequence was used as a template. The RNA product was resistant to S1 nuclease digestion (Fig. 4, lanes 5 and 6). However, S1 nuclease treatment after heat denaturation almost completely degraded the RNA (lane 7). This result indicated that the product formed by the RdRp reaction was double-stranded RNA.

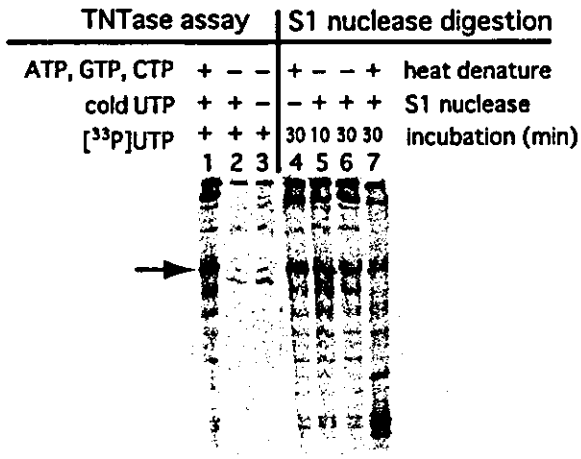

FIG. 4. TNTase assay and S1 nuclease digestion. An in vitro-transcribed RNA, 606-polyA, corresponding to the 3′-terminal 232 nucleotides of the NV genome, was used as a template for the RdRp reaction. For TNTase assays, reactions were performed without ATP, GTP, and CTP (lane 2) or without ATP, GTP, CTP, and cold UTP (lane 3). An RNA product from a standard reaction mixture is shown (lane 1) as a control. For the S1 nuclease digestion analyses, RdRp products were heat denatured at 95°C for 2 min (lanes 4 and 7) before treatment without (lane 4) or with (lanes 5, 6, and 7) S1 nuclease for the indicated times. The 232-nucleotide band, identified by an arrow, is missing from lanes 2, 3, and 7. RNA products were analyzed by methods similar to those described for Fig. 2.

Poly(A)- and primer-independent RdRp activity. The results described above indicated that NV RdRp was able to synthesize cRNA without the primer at the 3′ region of the NV genome. Since the NV genome contains a poly(A) sequence at the 3′ end (11, 15), we investigated whether the poly(A) sequence is required for the initiation of RNA synthesis by NV RdRp. RdRp activity was measured by using NV 3′ genomic RNA with or without a poly(A) tail. The 608-pA template RNA contained the 3′-terminal region of the NV genome and 30 nucleotides of poly(A) sequence; 608-delA RNA contained the same NV sequence but not the poly(A) sequence (Fig. 5A). [^{33}P]UTP incorporation was similar in both reactions. Furthermore, the labeled RNA size markers driven by T7 RNA polymerase confirmed that the RdRp product was the same size as the template RNA, irrespective of the presence of the poly(A) tail on the template (Fig. 5B). The results strongly indicated that the 3′ poly(A) sequence is not necessary for the initiation of synthesis or for synthesis to the exact length of the cRNA.

We next examined the influence on RdRp activity of the addition of an oligo(U)$_{15}$ primer or UpU dimer primer to the template RNA containing the poly(A) tail (Fig. 5C). When the oligo(U)$_{15}$ primer was added to the reaction, the amounts of RdRp product increased slightly with increasing amounts of primer. Also, a distinct RNA product was observed which migrated faster than the templates. The reason for the presence of this smaller RNA is not known. The presence of the oligo(U)$_{15}$ primer made little difference on the synthesis of the major product, which corresponded to cRNA of the template RNA (Fig. 5C, lanes 2 to 4). Interestingly, there was no effect on RNA production with the reaction containing the dinucleotide primer UpU (Fig. 5C, lanes 5 to 7). From these results, we concluded that NV RdRp could synthesize RNA comple-

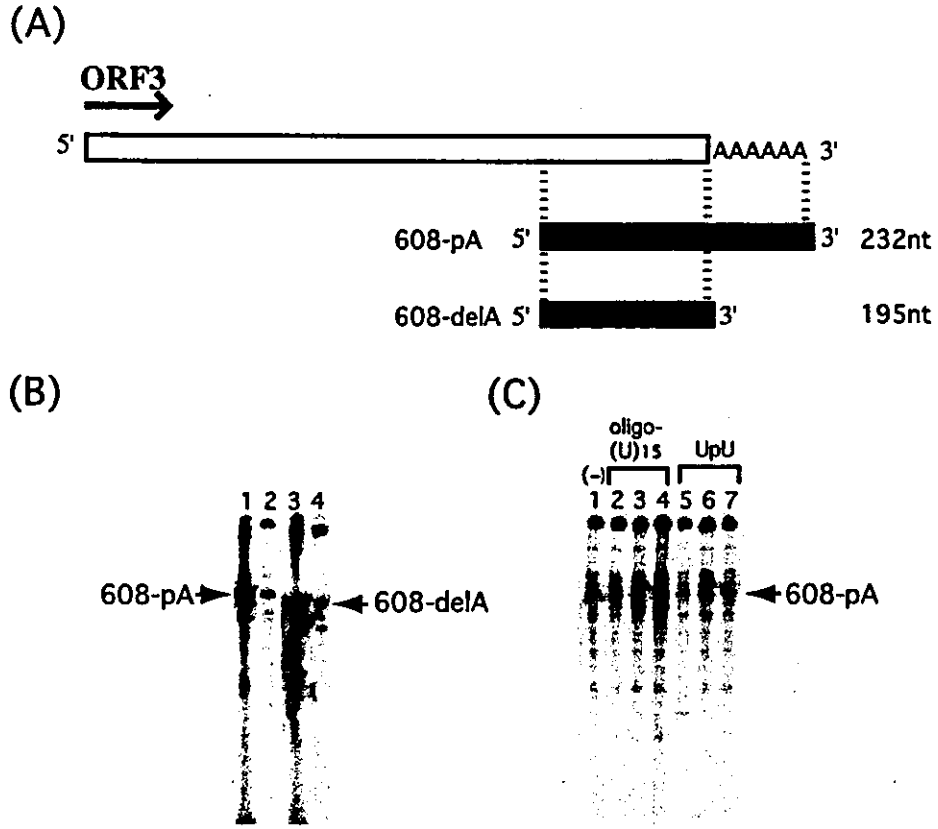

FIG. 5. RdRp activity was not dependent on RNA primer and poly(A) sequence. (A) Genome structure downstream of NV ORF3 with poly(A). The RNA templates used for RdRp assays are represented by black bars. (B) The RdRp products from reactions with template RNA 608-pA (lane 2) and 608-delA (lane 4), together with labeled RNA from a T7 polymerase reaction of 608-pA (lane 1) and 608-delA (lane 3), are represented. (C) Effect of RNA primer on RdRp activity. RdRp reactions were performed with 608-pA RNA as a template, with 1.0 pmol (lane 2), 5.0 pmol (lane 3), or 20.0 pmol (lane 4) of oligo$(U)_{15}$; 10.0 pmol (lane 5), 1.0 nmol (lane 6), or 10.0 nmol (lane 7) of UpU dinucleotide primer; or no primer (lane 1). RNA products were analyzed by methods similar to those described for Fig. 2.

mentary to the NV genomic RNA in a primer- and poly(A)-independent manner.

Effect of RdRp inhibitors. The assay system described above allowed us to screen for potential NV RdRp inhibitors. Various concentrations of gliotoxin or PAA, which inhibits the activities of other viral RdRp proteins, were added to the NV RdRp reaction. PAA inhibited the RdRp activity (Fig. 6). The estimated 50% inhibitory concentration of PAA for NV RdRp activity was <20 μM. No inhibitory effect was observed with gliotoxin, even at concentrations as high as 250 μM.

DISCUSSION

Previous studies of viral homology have indicated that the C terminus of NV ORF1 contains a motif in the RdRp that is conserved among various plus-strand RNA viruses. In this study, we report that the 3D region of the NV genome contains an active RdRp. We expressed a soluble recombinant RdRp encoded by the NV 3D genomic region in insect cells without a tagged sequence but with a single additional methionine residue at the N terminus. We purified the protein and established a system for measuring its RNA polymerase activity. That activity was not due to contamination by an endogenous

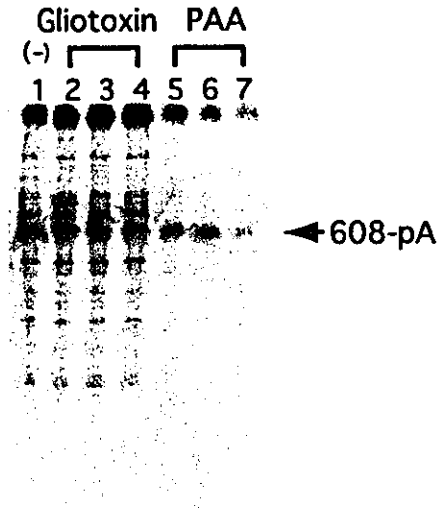

FIG. 6. Effects of RdRp inhibitors. RdRp reactions were performed with 608-pA RNA as a template, with 25 μM (lane 2), 100 μM (lane 3), or 250 μM (lane 4) gliotoxin; 25 μM (lane 5), 100 μM (lane 6), or 250 μM (lane 7) PAA; or no inhibitors. The 232-nucleotide band, identified by an arrow, disappeared gradually upon PAA treatment. RNA products were analyzed by methods similar to those described for Fig. 2.

insect polymerase, and actinomycin D did not inhibit the RdRp reaction, also indicating a lack of endogenous RdRp.

We focused on the conserved GDD motif in the 3D region. Found in most RdRps of positive-strand RNA viruses, GDD is important for metal binding and is considered to be the catalytic site of the enzyme (14). When we replaced the GDD motif in RdRp, the RNA polymerase activity was lost, and the expressed 3B protein of NV also lacked activity. The loss of RdRp activity in these mutant RdRp proteins indicated that labeled RNA products obtained by a reaction with the wild-type RdRp protein were driven by an RNA polymerase-related activity and maybe by an intrinsic activity of the expressed NV RdRp protein. The enzymatic activity of NV RdRp depended on Mn^{2+}: the optimal Mn^{2+} concentration was 2.0 mM. This requirement for divalent cations is similar to that of the primer-independent de novo RNA polymerase activity of poliovirus (1), HCV (18, 21), and human rhinovirus 16 (9). In the presence of Mn^{2+} ions, RdRp from RHDV is thought to form an active structure (19). Our observations suggest that Mn^{2+} ions promote conformational changes in NV RdRp that are similar to those of other positive-strand RNA viruses, such as picornaviruses, HCV, and RHDV. We believe that the enzymatic activity in the presence of Mn^{2+} may reflect a primary biological function of RdRp, and we used Mn^{2+} for all of our RdRp characterizations.

Several investigators have shown that in vitro viral RdRp reactions generate cRNA by a "copy-back" mechanism (3, 26). These reactions produce dimer-sized RNAs, presumably as a result of a self-priming event at the extreme 3′ terminus of the template. In our study, dimer-sized RNAs were not seen when the RdRp products were separated in denatured gels. We speculate that NV RdRp does not have a copy-back mechanism for cRNA synthesis. This notion is supported by the absence of self-priming by an additional oligo(U) at the 3′ end of the template RNA mediated by TNTase activity.

Interestingly, our results indicate that NV RdRp may not recognize poly(A). RNA production was as efficient without a poly(A) tail at the 3′-terminal region of the template RNA as it was with the tail. Furthermore, priming by synthetic oligo(U) or UpU had little effect on the RdRp activity. RdRp was able to synthesize cRNA without a poly(A) tail. Therefore, as reported for HCV RdRp (12), there must be a specific sequence requirement for *cis*-acting signals for RNA synthesis when NV genomic RNA is used. Additional studies are needed to determine the specific sequence.

Our results revealed that NV RdRp has the activity of de novo RNA synthesis with the NV genomic RNA as a template. Like those of other RNA viruses (1, 12, 18), NV RdRp directs minus-strand RNA synthesis in a primer-independent manner. We also showed an interesting feature of NV, namely that the activity of minus-strand synthesis is independent of a poly(A) tail. The NV genome encodes a VPg-like protein on the genome (11, 15). In picornaviruses, the VPg protein is thought to link to the 5′ end of the genome and serve as a primer for RdRp (23). In the *Caliciviridae*, a genome-linked VPg protein has also been reported for FCV (8). Therefore, it is important to determine whether the VPg protein is linked to the NV genome and has a role in cRNA synthesis.

Finally, our in vitro RdRp assay may be useful in further studies to develop drugs to treat NV, and the NV RdRp may itself be a useful target for antiviral drugs. It was strongly inhibited by PAA, which interferes with the replication of DNA viruses (4). The 50% inhibitory concentration (<20 μM) for NV RdRp was significantly lower than that reported for HCV RdRp (10), indicating a specific inhibition of NV RdRp activity by PAA. In contrast, gliotoxin, a known inhibitor of poliovirus and HCV RdRps (5, 22), had little effect on NV RdRp activity, despite the high concentrations tested. The differences in sensitivities may be attributed to the specific nature of NV RdRp, which synthesizes minus-strand RNA in a primer- and poly(A)-independent manner.

ACKNOWLEDGMENT

This work was supported by Research on Health Sciences Focusing on Drug Innovation grant KH51048 from the Japan Health Sciences Foundation.

REFERENCES

1. **Arnold, J. J., S. K. Ghosh, and C. E. Cameron.** 1999. Poliovirus RNA-dependent RNA polymerase (3D(pol)). Divalent cation modulation of primer, template, and nucleotide selection. J. Biol. Chem. **274**:37060–37069.
2. **Bartenschlager, R., and V. Lohmann.** 2000. Replication of hepatitis C virus. J. Gen. Virol. **81**:1631–1648.
3. **Behrens, S. E., L. Tomei, and R. De Francesco.** 1996. Identification and properties of the RNA-dependent RNA polymerase of hepatitis C virus. EMBO J. **15**:12–22.
4. **Binne, U. K., W. Amon, and P. J. Farrell.** 2002. Promoter sequences required for reactivation of Epstein-Barr virus from latency. J. Virol. **76**:10282–10289.
5. **Ferrari, E., J. Wright-Minogue, J. W. Fang, B. M. Baroudy, J. Y. Lau, and Z. Hong.** 1999. Characterization of soluble hepatitis C virus RNA-dependent RNA polymerase expressed in *Escherichia coli*. J. Virol. **73**:1649–1654.
6. **Fukushi, S., M. Okada, T. Kageyama, F. B. Hoshino, K. Nagai, and K. Katayama.** 2001. Interaction of poly(rC)-binding protein 2 with the 5′-terminal stem loop of the hepatitis C-virus genome. Virus Res. **73**:67–79.
7. **Green, K. Y., A. Z. Kapikian, and R. M. Chanock.** 2001. Human caliciviruses, p. 841–874. *In* D. M. Knipe, P. M. Howley, D. E. Griffin, et al. (ed.), Fields virology, 4th ed. Lippincott-Raven, Philadelphia, Pa.
8. **Herbert, T. P., I. Brierley, and T. D. Brown.** 1997. Identification of a protein linked to the genomic and subgenomic mRNAs of feline calicivirus and its role in translation. J. Gen. Virol. **78**:1033–1040.
9. **Hung, M., C. S. Gibbs, and M. Tsiang.** 2002. Biochemical characterization of rhinovirus RNA-dependent RNA polymerase. Antivir. Res. **56**:99–114.
10. **Ishii, K., Y. Tanaka, C. C. Yap, H. Aizaki, Y. Matsuura, and T. Miyamura.** 1999. Expression of hepatitis C virus NS5B protein: characterization of its RNA polymerase activity and RNA binding. Hepatology **29**:1227–1235.
11. **Jiang, X., M. Wang, K. Wang, and M. K. Estes.** 1993. Sequence and genomic organization of Norwalk virus. Virology **195**:51–61.
12. **Kao, C. C., X. Yang, A. Kline, Q. M. Wang, D. Barket, and B. A. Heinz.** 2000. Template requirements for RNA synthesis by a recombinant hepatitis C virus RNA-dependent RNA polymerase. J. Virol. **74**:11121–11128.
13. **Katayama, K., H. Shirato-Horikoshi, S. Kojima, T. Kageyama, T. Oka, F. Hoshino, S. Fukushi, M. Shinohara, K. Uchida, Y. Suzuki, T. Gojobori, and N. Takeda.** 2002. Phylogenetic analysis of the complete genome of 18 Norwalk-like viruses. Virology **299**:225–239.
14. **Koonin, E. V.** 1991. The phylogeny of RNA-dependent RNA polymerases of positive-strand RNA viruses. J. Gen. Virol. **72**:2197–2206.
15. **Lambden, P. R., E. O. Caul, C. R. Ashley, and I. N. Clarke.** 1993. Sequence and genome organization of a human small round-structured (Norwalk-like) virus. Science **259**:516–519.
16. **Li, T. C., Y. Yamakawa, K. Suzuki, M. Tatsumi, M. A. Razak, T. Uchida, N. Takeda, and T. Miyamura.** 1997. Expression and self-assembly of empty virus-like particles of hepatitis E virus. J. Virol. **71**:7207–7213.
17. **Liu, B. L., G. J. Viljoen, I. N. Clarke, and P. R. Lambden.** 1999. Identification of further proteolytic cleavage sites in the Southampton calicivirus polyprotein by expression of the viral protease in E. coli. J. Gen. Virol. **80**:291–296.
18. **Luo, G., R. K. Hamatake, D. M. Mathis, J. Racela, K. L. Rigat, J. Lemm, and R. J. Colonno.** 2000. De novo initiation of RNA synthesis by the RNA-dependent RNA polymerase (NS5B) of hepatitis C virus. J. Virol. **74**:851–863.
19. **Ng, K. K., M. M. Cherney, A. L. Vazquez, A. Machin, J. M. Alonso, F. Parra, and M. N. James.** 2002. Crystal structures of active and inactive conformations of a caliciviral RNA-dependent RNA polymerase. J. Biol. Chem. **277**: 1381–1387.
20. **Ranjith-Kumar, C. T., J. Gajewski, L. Gutshall, D. Maley, R. T. Sarisky, and C. C. Kao.** 2001. Terminal nucleotidyl transferase activity of recombinant *Flaviviridae* RNA-dependent RNA polymerases: implication for viral RNA synthesis. J. Virol. **75**:8615–8623.

21. **Ranjith-Kumar, C. T., Y. C. Kim, L. Gutshall, C. Silverman, S. Khandekar, R. T. Sarisky, and C. C. Kao.** 2002. Mechanism of de novo initiation by the hepatitis C virus RNA-dependent RNA polymerase: role of divalent metals. J. Virol. 76:12513–12525.
22. **Rodriguez, P. L., and L. Carrasco.** 1992. Gliotoxin: inhibitor of poliovirus RNA synthesis that blocks the viral RNA polymerase 3Dpol. J. Virol. 66: 1971–1976.
23. **Rueckert, R. R.** 1996. *Picornaviridae*: the viruses and their replication, p. 609–654. *In* B. N. Fields, D. M. Knipe, and P. M. Howley (ed.), Fields virology, 3rd ed. Lippincott-Raven, Philadelphia, Pa.
24. **Seah, E. L., J. A. Marshall, and P. J. Wright.** 1999. Open reading frame 1 of the Norwalk-like virus Camberwell: completion of sequence and expression in mammalian cells. J. Virol. 73:10531–10535.
25. **Sosnovtsev, S. V., M. Garfield, and K. Y. Green.** 2002. Processing map and essential cleavage sites of the nonstructural polyprotein encoded by ORF1 of the feline calicivirus genome. J. Virol. 76:7060–7072.
26. **Steffens, S., H. J. Thiel, and S. E. Behrens.** 1999. The RNA-dependent RNA polymerases of different members of the family Flaviviridae exhibit similar properties in vitro. J. Gen. Virol. 80:2583–2590.
27. **Vazquez, A. L., J. M. Martin Alonso, R. Casais, J. A. Boga, and F. Parra.** 1998. Expression of enzymatically active rabbit hemorrhagic disease virus RNA-dependent RNA polymerase in *Escherichia coli*. J. Virol. 72:2999–3004.
28. **Wei, L., J. S. Huhn, A. Mory, H. B. Pathak, S. V. Sosnovtsev, K. Y. Green, and C. E. Cameron.** 2001. Proteinase-polymerase precursor as the active form of feline calicivirus RNA-dependent RNA polymerase. J. Virol. 75: 1211–1219.

Arch Virol (2004) 149: 1673–1688
DOI 10.1007/s00705-004-0345-4

Archives of Virology
Printed in Austria

Detection of norovirus and sapovirus infection among children with gastroenteritis in Ho Chi Minh City, Vietnam

G. S. Hansman[1,2], L. T. P. Doan[1], T. A. Kguyen[1], S. Okitsu[1], K. Katayama[2], S. Ogawa[2], K. Natori[2], N. Takeda[2], Y. Kato[3], O. Nishio[3], M. Noda[4], and H. Ushijima[1]

[1]Department of Developmental Medical Sciences, Graduate School of Medicine, The University of Tokyo, Tokyo, Japan
[2]Department of Virology II, National Institute of Infectious Diseases, Tokyo, Japan
[3]Infectious Disease Surveillance Center, National Institute of Infectious Diseases, Tokyo, Japan
[4]Hiroshima City Institute of Public Health, Hiroshima, Japan

Received November 14, 2003; accepted March 22, 2004
Published online May 10, 2004 © Springer-Verlag 2004

Summary. This report describes norovirus (NoV) and sapovirus (SaV) infections in hospitalized children with acute sporadic gastroenteritis in Ho Chi Minh City, Vietnam. Stool specimens collected between December 1999 and November 2000 were examined for NoV and SaV using reverse transcription-PCR and phylogenetic analysis. NoVs were detected in 72 of 448 rotavirus-negative specimens, counted as part of an overall annual detection rate of 5.4% (72 of 1,339 children). This included four NoV genogroup I (GI) strains and 68 NoV GII strains. Only one SaV GI strain was detected in the rotavirus-negative specimens. Over 73% of the NoV sequences belonged to GII/4 (Lordsdale cluster) and were detected in all months except March. We also detected GII/3 strains (Saitama U201 cluster), a naturally occurring recombinant NoV, between January 2000 and March 2000 but not after this period. Other NoV strains belonging to GI/4, GI/8, GII/1, and GII/7 were also detected but were infrequent. In addition, two almost identical NoV GII strains (strains 026 and 0703) collected six months apart were classified into a new genotype that includes the Mc37 strain, which was previously shown to be a recombinant NoV. During this one-year study, the NoV prevailed at the end of the rainy season and the beginning of the dry season. Further epidemiological studies may be necessary to determine whether the GII/4 strains continue to dominant in this region.